Biophysical Journal
Article

Biophysical Society

Lipid Interactions and Organization in Complex Bilayer Membranes

Oskar Engberg,[1] Tomokazu Yasuda,[2,3] Victor Hautala,[1] Nobuaki Matsumori,[2,4] Thomas K. M. Nyholm,[1] Michio Murata,[2,3,*] and J. Peter Slotte[1,*]

[1]Biochemistry, Faculty of Science and Engineering, Åbo Akademi University, Turku, Finland; [2]Department of Chemistry, Graduate School of Science, Osaka University, Toyonaka, Osaka, Japan; [3]Lipid Active Structure Project, Japan Science and Technology Agency, ERATO, Toyonaka, Osaka, Japan; and [4]Department of Chemistry, Faculty of Science, Kyushu University, Fukuoka, Japan

ABSTRACT Bilayer lipids influence the lateral structure of the membranes, but the relationship between lipid properties and the lateral structure formed is not always understood. Model membrane studies on bilayers containing cholesterol and various phospholipids (PLs) suggest that high and low temperature melting PLs may segregate, especially in the presence of cholesterol. The effect of different PL headgroups on lateral structure of bilayers is also not clear. Here, we have examined the formation of lateral heterogeneity in increasingly complex (up to five-component) multilamellar bilayers. We have used time-resolved fluorescence spectroscopy with domain-selective fluorescent probes (PL-conjugated *trans*-parinaric acid), and ^{2}H NMR spectroscopy with site or perdeuterated PLs. We have measured changes in bilayer order using such domain-selective probes both as a function of temperature and composition. Our results from time-resolved fluorescence and ^{2}H NMR showed that in ternary bilayers, acyl chain order and thermostability in sphingomyelin-rich domains were not affected to any greater extent by the headgroup structure of the monounsaturated PLs (phosphatidylcholine, phosphatidylethanolamine, or phosphatidylserine) in the bilayer. In the complex five-component bilayers, we could not detect major differences between the different monounsaturated PLs regarding cholesterol-induced ordering. However, cholesterol clearly influenced deuterated *N*-palmitoyl sphingomyelin differently than the other deuterated PLs, suggesting that cholesterol favored *N*-palmitoyl sphingomyelin over the other PLs. Taken together, both the fluorescence spectroscopy and ^{2}H NMR data suggest that the complex five-component membranes displayed lateral heterogeneity, at least in the lower temperature regimen examined.

INTRODUCTION

Biological membranes consist of a complex mixture of different lipid species and various integral or associated proteins. The major lipid classes present are sphingolipids, glycerophospholipids, and sterols (1,2). The plasma membrane is enriched in sphingolipids and cholesterol, which are known to promote lateral separation in several model systems (3–5). In addition to lateral heterogeneity, the plasma membrane also has trans-bilayer heterogeneity, with sphingomyelin (SM) and glycosphingolipids in the outer leaflet and aminophospholipids (phosphatidylserine (PS), phosphatidylethanol-amine (PE)) in the inner leaflet (6). The transbilayer distribution of cholesterol in eukaryotic cells is not well understood, but a fluorescent sterol analog (dehydroergo-sterol) has been shown to preferentially partition into the inner leaflet (7).

As the sphingolipids of biological membranes have mainly saturated *N*-linked acyl chains (8), and the glycerolipids have mainly mono- and polyunsaturated acyl chains in their *sn*-2 position (1), the sphingolipids tend to form laterally segregated domains with high acyl chain order in both biological and model membranes. Glycerophospholipids may also segregate laterally to ordered domains if they are saturated (9), or into disordered domains if their acyl chains are highly unsaturated (10,11) The lateral segregation of SM, the most common sphingolipid in eukaryotic cell membranes, is stabilized in part by van der Waals interactions among the saturated acyl chains (12), by cholesterol-induced segregation into the liquid-ordered phase (13) and by interlipid hydrogen bonding between the SMs (14). Although cholesterol does not favor interacting with phospholipids (PLs) that have unsaturated acyl chain (15), cholesterol appears to prefer interacting with SM (16,17). Such favorable interactions are stabilized by van der Waals

Submitted October 6, 2015, and accepted for publication December 21, 2015.

*Correspondence: murata@chem.sci.osaka-u.ac.jp or jpslotte@abo.fi

Oskar Engberg and Tomokazu Yasuda contributed equally to this work.

Editor: Klaus Gawrisch.

http://dx.doi.org/10.1016/j.bpj.2015.12.043

interactions between the flat sterol ring system and the saturated acyl chains of SMs (18), and intermolecular hydrogen bonding (19). The side chain of cholesterol is also important for sterol/phospholipid interactions, as small changes to the isooctyl side chains will have marked weakening effects on the interaction between cholesterol and colipids (20–23).

The interaction of cholesterol with different PLs (e.g., phosphatidylcholines (PC), PE, and PS) in biological membranes is not fully understood. In model membrane systems, it has been observed that cholesterol interacts unfavorably with PE, possibly because the headgroup of PE is smaller than that of PC (24). The bilayer solubility of cholesterol in PE bilayers is also much lower (50%) than it is in acyl-chain-matched PC bilayers (66%) (25). Cholesterol partitioning studies suggest that cholesterol favors SM over other PLs (26,27), and PS over acyl-chain-matched PCs (27).

To detect the heterogeneities formed by the nonrandom mixing of lipids, different methods can be applied that have different spatial and temporal resolutions (28,29). Fluorescence spectroscopy can yield nanosecond and nanometer resolution, but the downside is that fluorescently labeled lipids often have bulky fluorophores that may affect lateral partitioning in unknown ways (30,31). The fluorescent fatty acid *trans*-parinaric acid (tPA), is, however, similar in size and properties to saturated acyl chains of PLs. The excited-state lifetime of tPA is very sensitive to changes in acyl chain order in its immediate vicinity (32,33). Thus, tPA appears to be a very valuable tool for studying the formation and properties of lateral domains, at least in model membrane systems (32–35).^{2}H NMR has been very useful for elucidating the behavior of lipids in bilayer membranes (36), and the advantage is the use of deuterated lipids whose behavior is very similar to that of native lipids (37,38). Unfortunately, the time resolution of ^{2}H NMR is not as good as that of time-resolved fluorescence spectroscopy, and hence the method can fail to directly detect changes in the most dynamic domains (28). For a detailed discussion on the time resolution of NMR, please refer to (39). However, the atomic resolution of ^{2}H NMR is superior to most other methods, and thus will be a valuable approach to study lipid properties in bilayer membranes.

In this study, we examined mutual interactions of cholesterol, SM, and glycerophospholipids (1-palmitoyl-2-oleoyl-*sn*-glycero-3-phosphocholine (POPC), 1-palmitoyl-2-oleoyl-*sn*-glycero-3-phosphatidylethanolamine (POPE), and 1-palmitoyl-2-oleoyl-*sn*-glycero-3-phosphoserne (POPS)) in multilamellar bilayer systems. We used ^{2}H NMR and time-resolved fluorescence spectroscopy to examine the bilayer order in increasingly complex bilayers in the presence of various cholesterol concentrations at different temperatures. For ^{2}H NMR, we used 9′,9′-d_2-palmitoyl SM or d_{31}-palmitoyl-perdeuterated PSM-d_{31}, POPC-d_{31}, POPE-d_{31}, and POPS-d_{31}. For time-resolved fluorescence spectroscopy, we used tPA-based probes: 1-oleoyl-2-tPA-*sn*-glycero-3-phosphocholine (O-tPA-PC), and *N*-tPA-sphingomyelin (tPA-SM). The former partitions preferentially into disordered phases (POPC/PSM bilayers: $K_p^{So/Ld}$ 0.35), whereas the latter prefers ordered phases (POPC/PSM bilayers: $K_p^{So/Ld}$ 1.7 (40)). Our experimental approach allows us to examine changes in lateral bilayer structure by using domain-selective fluorescent reporter molecules (time-resolved fluorescence analysis), and determine acyl chain ordering by ^{2}H NMR using site-specific or perdeuterated acyl chains in different PL species, as a function of temperature and cholesterol concentration. We show that five-component bilayers with PSM, POPC, POPE, and POPS in the presence of cholesterol show clear lateral heterogeneity, with coexisting ordered and disordered domains. In these complex bilayers, the PSM order appeared to be most affected by cholesterol up to the 20–25 mol% cholesterol range. The relevance of these findings will be discussed.

MATERIALS AND METHODS

Expanded materials and methods are provided in the Supporting Material.

RESULTS

Fluorescent domain-selective probes detect formation of ordered and disordered domains

The excited-state lifetime of tPA is very sensitive to lateral packing properties in its vicinity (32,33,41). We performed tPA lifetime measurements to examine the formation of lateral domains in bilayers composed of PSM, cholesterol, and one of the unsaturated lipids POPC, POPE, or POPS. Instead of free tPA, two PL derivatives were used: tPA-SM and O-tPA-PC. The SM derivative has been shown to mimic PSM partitioning between the gel and fluid phase well (40), and O-tPA-PC has a strong preference (stronger than POPC) for the fluid phase (POPC/PSM bilayers $K_p^{So/Ld}$ 0.35; Fig. S1 in the Supporting Material). With these probes we therefore could monitor changes in the acyl chain order in PSM-rich and unsaturated PL-rich environments, respectively. All fluorescence lifetime components are listed separately in Tables S1–S3.

We measured the fluorescence decays of the two domain-selective probes (tPA-SM and O-tPA-PC) in the binary and ternary lipid mixtures at different temperatures (for typical emission decay curves of tPA-SM in POPC/PSM/Chol bilayers, see Fig. S2). The binary membranes were composed of one of the PLs (PSM, POPC, POPE, or POPS) and cholesterol, and the ternary systems consisted of PSM, one of the unsaturated PLs (POPC, POPE, or POPS), and cholesterol. In the binary system composed of the unsaturated lipids and cholesterol, the average lifetimes of O-tPA-PC at 20°C was highest in POPC/Chol (~13.5 ns, Fig. 1 *A*), intermediate in POPE/Chol (12.5 ns, Fig. 1 *B*), and lowest in POPS/Chol (10.5 ns; Fig. 1 *C*). As the temperature was increased, the average fluorescence lifetimes of O-tPA-PC

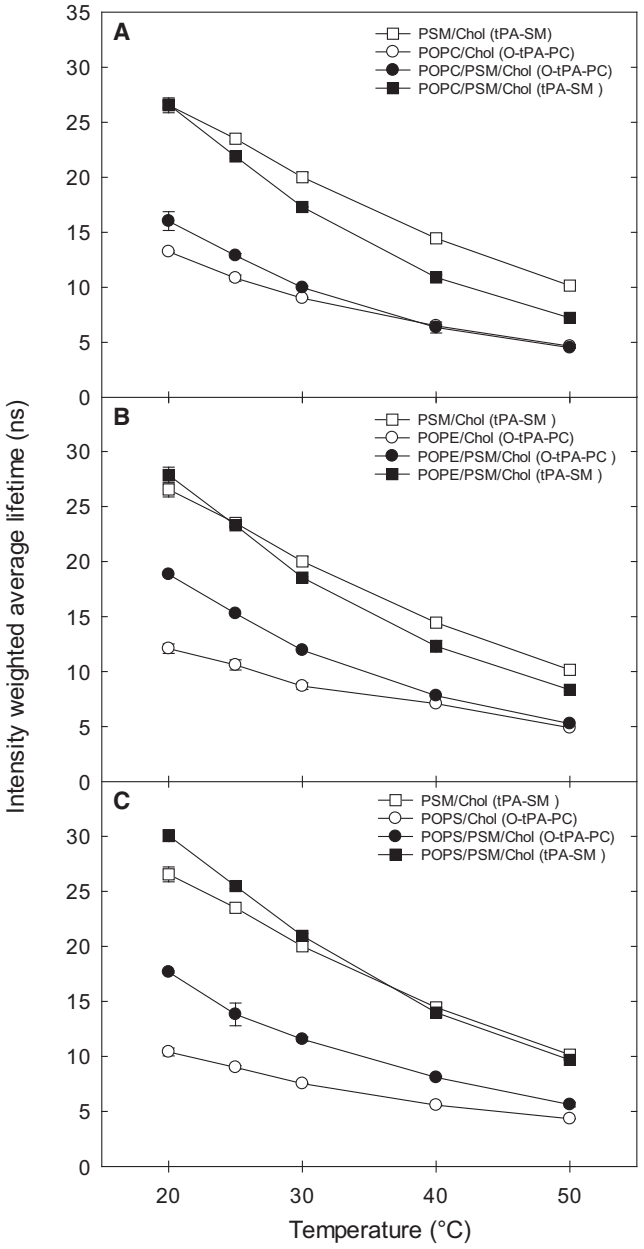

FIGURE 1 Detection of membrane order by average lifetime of domain-selective probes as a function of temperature in binary and ternary bilayers. 1 mol% of either tPA-SM (*measuring order in the ordered domain*) or O-tPA-PC (*measuring order in the disordered domain*) was included in the bilayers. The ternary bilayers (*black*) contained PSM/POPX/Chol (34.5: 34.5: 30 mol%) and the binary bilayers (*white*) contained POPX/Chol or PSM/Chol (53: 47 mol%). (*A*) shows data for POPC mixtures, (*B*) for POPE, and (*C*) for POPS mixtures; all panels included a comparison to the PSM/Chol mixture. Values are average ± SD of $n = 3$ (error bar may be smaller than symbol). For more details on the lifetimes, see Tables S1 and S2.

decreased in all three systems, to ~4.5–5 ns at 50°C (Fig. 1). In the binary PSM/Chol bilayers, the average fluorescence lifetime of tPA-SM was markedly longer than that of O-tPA-PC in the unsaturated binary bilayers. This difference was not an effect of the different probes used, since similar results were obtained using O-tPA-PC in the binary PSM/Chol bilayers and tPA-SM in the disordered unsaturated bilayers (Table S1).

In the ternary systems we measured the fluorescence lifetimes of tPA-SM and O-tPA-PC. At 20°C, the tPA-SM probe reported similar average lifetimes in the ternary bilayers as in the binary bilayers (Fig. 1), suggesting that the order in the PSM-rich domains (in all three ternary systems) were similar to that in the binary PSM/Chol, agreeing with earlier NMR results comparing the ordered phase in ternary 1,2-dioleoyl-*sn*-glycero-3-phosphocholine (DOPC)/*N*-stearoyl-sphingomyelin (SSM)/Chol to binary SSM/Chol bilayers (42). However, when O-tPA-PC was used to probe the order in the unsaturated PL environment at 20°C, the average lifetime was increased in the ternary system compared to the corresponding binary bilayers (Fig. 1), likely arising from effects of PSM on the order of unsaturated PL-rich domains and partitioning of the probe into ordered domains. As the temperature was increased, the difference between the binary and ternary system reported by O-tPA-PC disappeared (Fig. 1). The average lifetime of tPA-SM in ternary bilayers, containing POPC or POPE, decreased clearly below the lifetime observed in the binary PSM/Chol system when the temperature was increased. In the ternary system with POPS the average lifetime of tPA-SM was similar to that of the binary PSM/Chol systems at 50°C. However, as the lifetime in this system seems to be high throughout the temperature range, it is likely due to different probe behavior in POPS containing bilayers. Furthermore, the effect of elevated temperature was larger on tPA-SM than on O-tPA-PC in the ternary systems, suggesting that the tPA-SM sensed ordered lateral domains at lower temperatures, and that these gradually melted as the temperature increased. Interestingly, in the ternary bilayers with tPA-SM, an additional long-lifetime component was required to fit the decay curves at 20, 25, and 30°C in all systems (Fig. 2). This further supports the assumption that the SM-based probe sensed a more ordered environment than the PC probe.

^{2}H NMR measurements of labeled PSM in binary and ternary lipid bilayers

To further explore how the different unsaturated lipids (POPC, POPE, and POPS) influenced the formation of lateral domains in binary and ternary lipid bilayers, we performed ^{2}H NMR experiments with PSM deuterated at the 9′ carbon in the palmitoyl chain (9′,9′-d_2 -PSM). This position was chosen, because cholesterol has been shown to have the largest effect on the SM acyl chain order around this position (17,36). The order of the deuterated carbon in position 9 can be discerned from the width between the peak doublets (Pake pairs). In the absence of cholesterol, the PSM/POPX molar ratio in the binary multilamellar vesicles

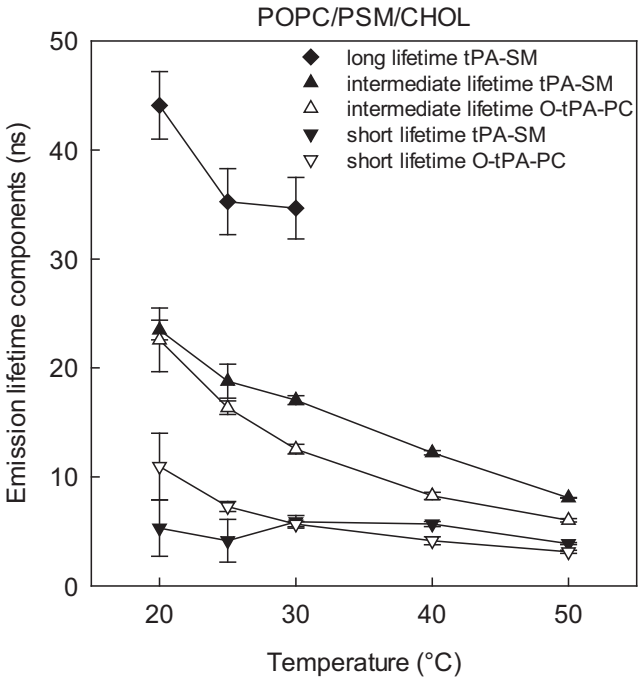

FIGURE 2 Lifetime-components of the tPA fluorescence decays in PSM/POPC/CHOL bilayers. 1 mol% of either tPA-SM (detecting order in the ordered domain) or O-tPA-PC (detecting order in the disordered domain) was included in the bilayers. The bilayers contained PSM/POPC/Chol (34.5: 34.5: 30 mol%). Each value is the average ± SD of $n = 3$–5. For more details on the lifetimes, see Table S2.

(MLVs) was 1:2, whereas with cholesterol the composition became PSM/POPX/Chol 1:2:1 (by mole). ^{2}H NMR spectra recorded at 30°C with the different systems are shown in Fig. 3. In the absence of cholesterol, spectra obtained with PSM/POPE bilayers showed markedly larger quadrupole splitting ($\Delta\nu$) than with the other binary mixtures (Fig. 3 *A*). The smallest $\Delta\nu$ was observed with PSM/POPC bilayers. This indicated that the acyl chain order in these binary PL bilayers increased in the order POPC < POPS < POPE, which is what would be expected based on the order observed in pure POPC, POPS, and POPE bilayers (43).

The addition of cholesterol to all systems led to wider spectra (increased acyl chain order), in agreement with previously reported results (44). After cholesterol was added, the $\Delta\Delta\nu$ of 9′,9′-d_2-PSM was largest for the POPC/PSM ternary bilayers followed by POPS/PSM and last POPE/PSM bilayers (Fig. 3 *B*). In all the spectra 9′,9′-d_2-PSM shown in Fig. S2 (and spectra at other temperatures, not shown) there clearly was only one major Pake pair. This indicates that possible lateral domains in the lipid bilayers were not long lived enough or too dynamic to give rise to a separate Pake pair on the NMR timescale.

The lateral heterogeneity in the ternary bilayers was further assessed by plotting the $\Delta\nu$ reported by 9′,9′-d2-PSM in the different lipid compositions as a function of temperature. When $\Delta\nu$ of 9′,9′-d_2-PSM was plotted as a function of temperature, the acyl chain order, as deduced from the $\Delta\nu$, decreased in all ternary bilayers as well as in binary PSM/Chol (1:1) bilayers with increased temperature (Fig. 3 *C*). The binary PSM/Chol bilayers had a high acyl chain order at 20°C and the order decreased only modestly as the temperature increased. If the ordered domains in the ternary bilayers were composed of only PSM and cholesterol, a similar acyl chain order would be expected in the

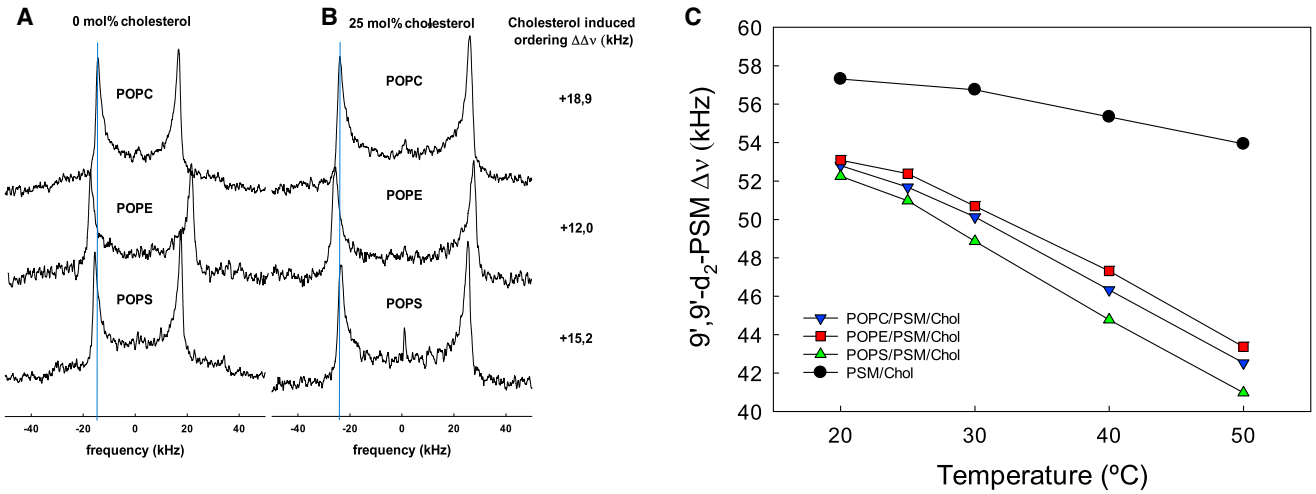

FIGURE 3 Effect of cholesterol and different monounsaturated PLs on ^{2}H spectra of 9′,9′-d_2-PSM at 30°C (*A* and *B*), or as a function of temperature (*C*). MLVs were prepared to 50% hydration with the composition 9′,9′-d_2-PSM/POPX (1:2) shown in panel *A* and the composition 9′,9′-d_2-PSM/POPX/Chol (1:2:1) shown in panel *B*. The POPX lipid present in each spectrum is highlighted over each spectrum. The $\Delta\nu$ of 9′,9′-d_2-PSM in the presence of cholesterol minus the $\Delta\nu$ of 9′,9′-d_2-PSM in the absence of cholesterol ($\Delta\Delta\nu$) is indicated to the right of the spectra. In panel *C*, the quadrupole splitting values ($\Delta\nu$) of 9′,9′-d_2-PSM in binary or ternary bilayers composed of PSM/Chol or POPX/PSM/Chol is shown as a function of temperature. To see this figure in color, go online.

ternary system. This was not the case, and in all ternary bilayers, 9′,9′-d_2-PSM reported a lower acyl chain order in the ternary system than in the binary system at all temperatures. However, the relative decrease in order as a function of temperature was larger in the ternary systems than in the binary PSM/Chol bilayers. Although data from binary and ternary bilayers may not be directly compared, these temperature sensitivities suggest an increased presence of PSM-enriched ordered domains in the ternary bilayers at lower temperatures, in agreement with the observations with the tPA-phospholipid probes (Fig. 1), and previously published data (45). Thus, it seems that the lateral lipid organization in all the ternary systems was heterogeneous, i.e., ordered and disordered domains coexisted at least at the lower end of the temperature interval. When the temperature functions of $\Delta\nu$ from 9′,9′-d_2-PSM in membranes were compared with different unsaturated PL components, it appears that the three different PLs (POPC, POPE, and POPS) had similar influence on the order of the PSM acyl chains throughout the temperature range.

^{2}H NMR experiments with complex bilayer compositions

We then systemically examined lipid interactions in even more complex bilayers, composed of four PLs (PSM/POPC/POPE/POPS, 22:44:17:17) and various amounts of cholesterol. For simplicity we will call these "complex bilayers." The composition was chosen because it is close to the average total PL composition of plasma membranes in most cells (1). The effect of temperature and cholesterol content on the acyl chain order in the different lipids was determined by comparing the spectra of deuterium-labeled PSM (PSM-d_{31}), POPC (POPC-d_{31}), POPE (POPE-d_{31}), and POPS (POPS-d_{31}). The spectra recorded with the perdeuterated lipids were complex (Fig. S3), showing multiple overlapping Pake doublets arising from the different methylene and methyl groups within the perdeuterated acyl chains (as shown previously in many studies (37,44,45)). To enhance the resolution, the spectra were dePaked (Fig. S4). The spectra from all samples seem to have only a single Pake pair (similar to ternary 9′,9′-d_2-PSM spectra) for each position along the acyl chains, suggesting that possible lateral domains in the lipid bilayers were too dynamic to show up on the NMR timescale.

To analyze the effect of cholesterol and temperature on the acyl chain order in the deuterium-labeled lipids, the first spectral moment (M_1) was calculated for each spectrum (Fig. 4). This parameter is useful when analyzing liquid membranes because it is proportional to the average acyl chain order (45). The effect of cholesterol on the acyl chain order in the lipid bilayers was studied by including 0–31 mol% cholesterol in the samples, and measuring the ^{2}H NMR spectra of all the different deuterium-labeled lipids separately at temperatures between 20°C and 50°C (see

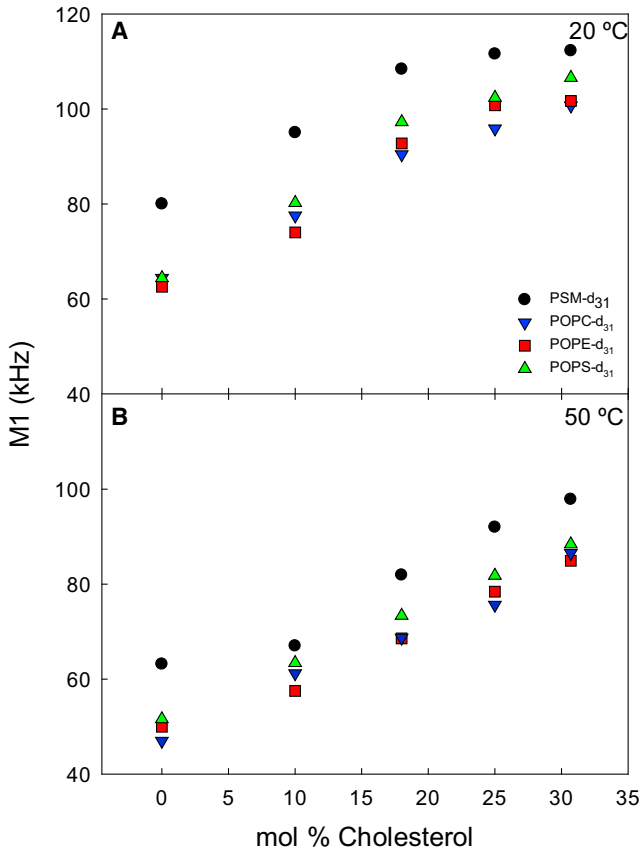

FIGURE 4 Cholesterol-induced ordering of perdeuterated lipids in complex bilayers at 20°C (*A*) and 50°C (*B*). Ordering was measured as the first spectral moment (M_1). MLVs were prepared to 50% hydration with the composition PSM/POPC/POPE/POPS 22:44:17:17 with the addition of 10–31 mol % cholesterol. To see this figure in color, go online.

Fig. S3 for spectra at 20°C for complex bilayers with variable cholesterol concentrations; Figs. S5 and S7 show M_1 for complex bilayers as a function of temperature or cholesterol, respectively; Fig S6 shows M_1 for pure perdeuterated PLs as a function of temperature). In Fig. 4, the effect of cholesterol on M_1 is shown for the lowest and the highest temperature. At all cholesterol concentrations and temperatures, PSM-d_{31} had substantially larger values of M_1 than the unsaturated lipids (which all had very similar M_1). For all the lipids, the addition of cholesterol increased the acyl chain order as seen from an increased M_1 (and broader spectra; Fig. S3). For PSM-d_{31} the ordering effect of cholesterol most clearly reached a plateau region at 18–25 mol% cholesterol, up to 40°C (Fig. S7). For the unsaturated lipids, M_1 increased more monotonously with increasing cholesterol at all temperatures. This result suggests that most of the PSM in the bilayer was affected by cholesterol already at 18–25 mol % cholesterol, whereas the monounsaturated PL molecules were less affected at these cholesterol concentrations at lower temperatures.

To get more insight into the lateral organization in the lipid bilayers, we plotted the acyl chain order (as M_1)

against temperature with all the cholesterol concentrations (Figs. 5 and S5). By comparing how the acyl chain order of different lipids in a complex bilayer was affected by changes in temperature, one can draw conclusions regarding the presence of specific lipids in ordered and disordered domains (45). The temperature dependence of M_1 (difference between M_1 at 50°C and 20°C) for PSM-d_{31} changed with the addition of cholesterol (10 mol %), as observed by a substantial increase in M_1 at 20°C but only a slight increase at 50°C (Figs. S5 and S7). Because the temperature dependence of M_1 for the other lipids was not influenced markedly by inclusion of 10 mol % cholesterol, it seems that cholesterol is interacting foremost with PSM when present in low quantities. At higher cholesterol concentrations, the difference between M_1 for PSM-d_{31} at 20°C and 50°C became smaller (this can be observed as a more flat line at 25 and 30 mol % cholesterol, Fig. S5). Because the molar concentration of cholesterol in these membranes exceeded that of PSM, this effect on the temperature dependence seems logical. Similar temperature dependencies of M_1 for POPE-d_{31} and POPS-d_{31} were found as in PSM-d_{31} bilayers. There was a substantial increase in M_1 at low temperatures, but only a slight increase at 50°C, and the cholesterol dependency was slightly different (Fig. S5). At higher cholesterol content, POPE-d_{31} and POPS-d_{31} showed less temperature dependency (more horizontal line), in part similar to that seen with PSM-d_{31}. POPC-d_{31} showed smoother temperature dependence with the addition of cholesterol.

Time-resolved fluorescence of tPA derivatives in complex bilayer membranes

To complement the ^{2}H NMR results obtained with the complex membranes, time-resolved fluorescence measurements using tPA-SM and O-tPA-PC were performed with similar PL compositions without or with cholesterol (31 mol %). The average fluorescence lifetimes observed with tPA-SM and O-tPA-PC at different temperatures is shown in Fig. 6. Up to ~30°C, the average lifetime of tPA-SM was significantly longer (taking into account probe differences in Table S1) than that of O-tPA-PC in cholesterol-free complex bilayers, suggesting that the probes reported properties of different lateral domains. This interpretation is supported by the need to add an additional long-lifetime component for fitting tPA-SM lifetime data for complex bilayers measured at low temperatures (Fig. 2; Table S3). A gel phase rich in PSM and POPE (46) likely existed at these temperatures. Gradually, as the temperature increased, the average fluorescence lifetimes of tPA-SM and O-tPA-PC in cholesterol-free complex bilayers became more similar as in a single phase bilayer. Altogether, these results suggest that at higher temperatures the probes were in a similar environment, indicating that lateral domains were not present, or were not detected by the probes.

The addition of cholesterol to the complex bilayers influenced the average fluorescence lifetimes of tPA-SM (from 13 to 22 ns at 20°C, Fig. 6) and O-tPA-PC (from 7 to 14 ns at 20°C, Fig. 6). However, at least at the lower end of the temperature range the lifetime of tPA-SM was significantly longer than that of O-tPA-PC, suggesting that with decreasing temperature the probes were increasingly separated from each other into different lateral lipid domains with different degrees of acyl chain order. An additional long-lifetime component was required to achieve good fits to the fluorescence decays at 25°C and 20°C t of tPA-SM at 25°C and 20°C that were not observed at higher temperatures (Fig. 2), which supports the assumption that this probe to a higher extent was present in ordered domains than the PC-based probe. It is noteworthy that amplitudes of the longest lifetime components were significantly higher in the presence of cholesterol than without (Table S3). This could be due to a larger amount of, or more stable ordered domains in cholesterol containing bilayers.

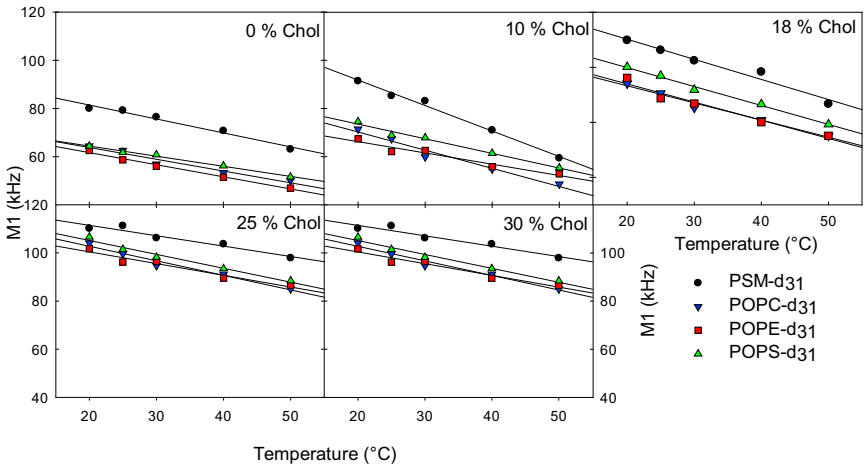

FIGURE 5 Cholesterol-induced ordering of perdeuterated lipids in complex bilayers as a function of temperature. Ordering was measured as the first spectral moment (M_1). MLVs were prepared to 50% hydration with the composition PSM/POPC/POPE/POPS 22:44:17:17 with the addition of 10–31 mol % cholesterol. The lines are only a guide. To see this figure in color, go online.

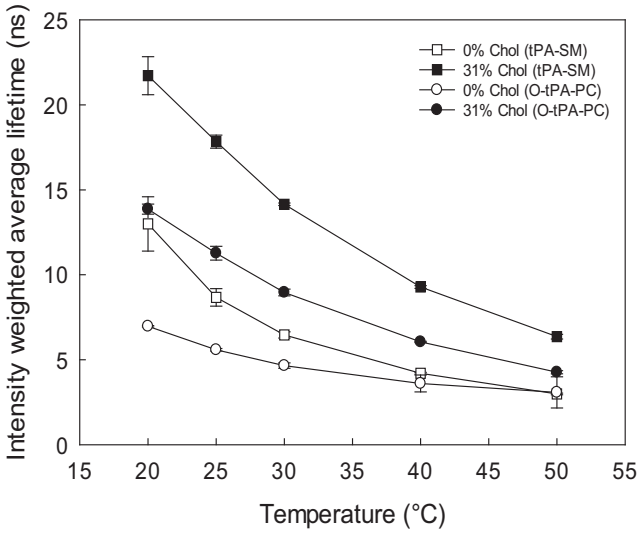

FIGURE 6 Effect of cholesterol on the average lifetime of the domain selective probes in complex bilayers as a function of temperature. 1 mol % tPA-SM (measuring order in the ordered domain) or O-tPA-PC (measuring order in the disordered domain) was included in the bilayers. MLVs were prepared with the composition PSM/POPC/POPE/POPS 22:44:17:17 without cholesterol and the cholesterol samples had an additional 31 mol % cholesterol. Each value is average ± SD of $n = 3$. For more details on the lifetimes, see Table S3.

DISCUSSION

Lateral heterogeneity and the formation of lateral domains in cellular membranes are thought to be part of the regulatory machinery in cells (3). In this work, we examined how different PLs and cholesterol affect the formation of ordered and disordered domains in binary, ternary, and five-component complex bilayers. Information about lateral organization in the model membranes was obtained using two methods: time-resolved fluorescence spectroscopy and ^{2}H NMR. In the time-resolved fluorescence experiments the fluorescence lifetime of tPA was measured. The fluorophore tPA (free fatty acid) is a useful tool as the acids fluorescence lifetime is strongly influenced by the acyl chain order in the surrounding lipid bilayer, and in addition partitions strongly into ordered lateral domains (32). Thus, the probe has been used especially in studies on gel phase formation (34,47), but it has also proven to be sensitive to the presence of the liquid-ordered phase (41). We prepared two different tPA-derived probes to alter their phase preference. The O-tPA-PC probe has a preference for the disordered phase (POPC/PSM bilayers: $K_p^{So/Ld}$ 0.35, Fig. S1) and reports changes in degrees of order from that phase, whereas tPA-SM preferentially partitions into ordered phases (POPC/PSM bilayers: $K_p^{So/Ld}$ 1.7) (40), and also partitions into cholesterol-enriched phases (41,48). In the POPC/PSM bilayers, the two PL probes partitioned similarly as their nonfluorescent counterparts (POPC and PSM) between the gel and liquid crystalline phases, and we assume that this is also true in the case of partitioning between the liquid-ordered and liquid crystalline phases.

To observe whether tPA reports different lifetimes when attached to lyso-SM than when linked to O-lyso-PC, we measured the lifetimes of both probes in the same environment (Table S1). In fluid POPC bilayers, the difference in lifetime between tPA-SM and O-tPA-PC was very small (Δ1.5 ns) at 20°C. In more ordered bilayers such as POPC/Chol, the difference was still small (Δ5 ns) between the probes. In PSM/Chol the difference was larger (Δ10 ns). Nevertheless, the difference between POPC/Chol and PSM/Chol bilayers was significant. The disordered nature of the ternary and the complex bilayers appeared to make the difference smaller between the probes, compared to measurements in the ordered binary bilayers (Table S1). The number of lifetime components was not dependent on the tPA-probe used but on the bilayer composition in the binary bilayers, therefore the different partitioning of the tPA-probes in ternary bilayers determined the requirement of additional lifetime components.

In the ^{2}H NMR experiments the deuterium-labeled lipids were structurally more similar to the unlabeled lipids than the tPA-lipids, which means that they mimic the partitioning behavior of their unlabeled counterparts even better than the fluorescent analogs. ^{2}H NMR has also been successfully used to investigate the lateral membrane structure in the past (42,45,49). However, the time resolution of the NMR experiments is not on par with the time resolution of fluorescence spectroscopy. This renders the NMR approach less likely to identify lateral domains if the interdomain lipid exchange is fast, or domain sizes are small. In this sense the time-resolved fluorescence approach has an advantage as the time frame is in the nanosecond range.

The recorded NMR spectra do not show separate peaks for the ordered and disordered domains, but instead a concentration weighted average of the two domains (Figs. 3, S3, and S4). This finding should indicate that ordered domains are small enough to allow lipid probe diffusion on the NMR timescale of submilliseconds. Similar observations have been made previously with ^{2}H NMR (4,10,45). However, with certain lipid compositions and at low temperatures, separate spectra from two coexisting domains have also been observed (4,50,51) According to several phase diagrams, both the composition used in the ternary bilayers in ^{2}H NMR and the time-resolved fluorescence approach, should be in the coexistence region of liquid-ordered phase and liquid crystalline phase (5,52,53). In the tPA lifetime experiments, the presence of two separate lateral domains was observed more clearly because at least in the ternary systems a third long-lifetime component had to be added to achieve a good fit to the tPA-SM decays while two shorter lifetimes were enough to fit the O-tPA-PC decays (Fig. 2; Table S2). Note that in the PSM/Chol membranes, both probes included a long third lifetime component (Table S1). This long-lifetime component suggests that a

significant fraction of the SM analogs exists within a more ordered lipid environment than the PC analogs (41). This further suggests that the timescale for lipid exchange between lateral domains in our system is slow enough to be detected with a nanoscale method but is too fast for the ^{2}H NMR timescale. The lipid exchange between domains could be different depending on the low and high temperature melting lipid used because the substructure of the liquid-ordered phase could differ depending on the lipids used to form the phase (54,55). Detection of double Pake pairs could also be related to the size of the domains as systems with SSM/DOPC/Chol (1/1/1) clearly showed two Pake pairs (42). The discrepancy could be explained by the difference in unsaturation between DOPC and POPC, causing micro- or nanoscopic phase separation as has been reported for systems that contain cholesterol/distearoylphosphatidylcholine (56).

Although the ^{2}H NMR and fluorescence data obtained at higher temperatures did not clearly show separate domains as discussed previously, the results still have features that suggest the presence of a lateral structure in the membranes. When the ^{2}H NMR and fluorescence data were plotted as a function of temperature, it was clear that the labeled molecules with a preference for the disordered domain responded differently to changes in temperature than those with a preference for ordered domains (Figs. 5, 6, and S5), and that the difference between the measured parameters with the different probes was largest at the lowest temperature. Our interpretation of this is that at low temperatures, there are two clearly distinct lateral types of domains, ordered and disordered, and the degree to which the labeled molecules sense these domains depends on their respective presence in a particular domain/phase. Thus, tPA-SM and PSM-d_{31} with a preference for ordered membrane domains were expected to report foremost the properties of ordered domains while O-tPA-PC, POPC-d_{31}, POPE-d_{31}, and POPS-d_{31} were expected to report primarily the properties of disordered domains.

For the ternary systems, the ^{2}H NMR data indicates that all three unsaturated PLs affected the deuterium-labeled PSM similarly (Fig. 3). This may be taken as an indication that the lateral organization in the bilayers is not influenced markedly by the headgroup structure in unsaturated lipids, as has been suggested previously (57). However, it seems that the degree of order reported by 9′9′-d_2-PSM was affected more in bilayers that contained POPS than in the other systems, which may be due to differences in the lipid compositions of the lateral domains.

The average tPA-SM fluorescence lifetimes also had a similar dependence on temperature in all three ternary systems, suggesting that the thermostability of the ordered domains was similar in all systems. The longest lifetime components (and the average lifetimes) for tPA-SM found in the bilayers that contained POPS were markedly longer than in the other systems (Table S2). Because the longest lifetime component should indicate the degree of order in the most ordered environment in the system, it seems that the ordered domains in the bilayers that contained POPS were more ordered than in the other two systems. POPS seemed to affect PSM differently in the nanosecond and microsecond scales. Looking at the lifetimes of O-tPA-PC in the same ternary systems, the longest average lifetimes and lifetime components were found in membranes that contained POPE followed by POPS and POPC, which would suggest that the disordered domains in the POPE bilayers would have the highest acyl chain order in this system (out of the three systems). This would agree with the fact that pure POPE bilayers have a higher acyl chain order than POPC and POPS membranes (Fig. S6; Table S2) and that PSM order was least disordered by POPE (Fig. 3 *A*) (43). However, the observed differences in the average lifetime and individual lifetime component lengths were likely also influenced by how O-tPA-PC partitioned between the ordered and disordered domains in the different lipid systems.

In the complex five-component bilayers, the use of perdeuterated PLs allowed us to gain information about the possible formation of lateral segregation (into ordered and disordered domains) in such complex bilayers. When the ^{2}H NMR data were plotted as a function of cholesterol (Figs. 4 and S7), it was clear that at lower temperatures the increase in order was not linear, but seemed to reach a plateau after first increasing linearly with the cholesterol content. As this behavior is most clear with PSM-d_{31}, our interpretation is that the ordering effect of cholesterol affected the SM more than the other PLs within the cholesterol concentration range. In turn, this would suggest that lateral domains enriched in cholesterol and PSM formed in the complex bilayers. At higher temperatures, the response to the increasing cholesterol content was more linear (Fig. S7), indicating that no lateral heterogeneity could be detected with ^{2}H NMR at 50°C.

Another approach for detecting lateral heterogeneity in lipid bilayers, which allowed comparison of the different lipids, was to plot the measured acyl chain order (presented as M_1) as a function of temperature. When this was done (see Figs. 5 and S5), it was clear that different deuterium-labeled lipids responded differently to changes in temperature at different cholesterol concentrations. At 10 mol % cholesterol the temperature altered the M_1 of PSM-d_{31} more than was seen without cholesterol. The M_1 temperature functions of the other lipids remained similar to that observed without cholesterol. This suggests that lateral domains enriched in PSM and cholesterol were formed at the lower temperatures. When the cholesterol concentration was increased to 18 mol %, the M_1 temperature functions recorded for POPE-d_{31} and POPS-d_{31} were altered. Thus, it may be assumed that at this cholesterol concentration, POPS and POPE were also affected more by cholesterol than POPC. When the cholesterol concentration was

increased further, the M_1 temperature functions again became flatter (less difference between the high and low temperatures), showing that POPS, POPE, and PSM lipids were affected by cholesterol at higher concentrations. This could be related to results from the ternary phase diagram that have shown that the affinity of cholesterol for the liquid-ordered phase is highest at a low cholesterol concentration and decreases at higher cholesterol concentrations (53,58) The M_1 of POPC-d_{31} remained unchanged by temperature throughout the cholesterol concentration range, possibly due to less incorporation into the ordered domains, or as a consequence of the higher molar ratio of this lipid present in the bilayers. Studies of the same systems with tPA-SM and O-tPA-PC gave similar results (Fig. 6). The difference in average fluorescence lifetime observed with the two probes at temperatures close to the physiological temperature suggested lateral domains were present in the membranes.

The ternary systems with SM and POPE formed ordered domains (Fig. 1; Table S2), and they may have contained cholesterol, which most likely interacted with SM and not PE, because PE is not known to form cholesterol-rich domains on its own (19). When PE is forced to interact with cholesterol in binary bilayers, cholesterol solubility (x-ray (25)) and cholesterol-induced ordering (Table S2) are reduced compared to PC/Chol bilayers (25,59,60). Cholesterol prefers to interact with saturated acyl chains, and the sphingosine backbone of SM is known to increase bilayer affinity for cholesterol (22). Even in ternary systems, the saturated 1,2-dipalmitoyl-*sn*-glycero-3-phosphoethanolamine and 1,2-dipalmitoyl-*sn*-glycero-3-phospho-L-serine or palmitoyl-ceramide-PE and palmitoyl-ceramide-PS were not able to form cholesterol-rich domains in an unsaturated PC bilayer (19,61). Cholesterol partitioning studies have examined unsaturated PE and PS bilayers and concluded that cholesterol affinity to different PLs was in the order PS > PC > PE (27). Diphenylhexatriene quenching has shown that POPE increased the thermostability of cholesterol-rich domains in POPE/PSM/Chol compared to POPC/PSM/Chol (60), which disagrees with our results. Although the variation in the headgroup in the monounsaturated lipid in the ternary bilayers did not affect the formation and thermostability of the PSM-rich domains in our ternary bilayers, polyunsaturation could affect how different headgroups affect domain formation and thermostability (11). In asymmetric biological plasma membranes, PS and PE do not have such high probability to interact with PSM, because of their different leaflet-localization. However, under some conditions, SM may be found in the inner leaflet and could influence aminophospho-lipid/cholesterol interactions (62). During apoptosis, PS transbilayer distribution is lost and PS will also be found in the outer leaflet (63) and could then interact with PSM.

Taken together, our results from time-resolved fluorescence and ^{2}H NMR in ternary and complex five-component bilayers have shown that laterally distinct ordered and disordered domains can be formed at certain compositions and temperature intervals. The ordered domains were invariably SM-rich, whereas the monounsaturated PLs were most prevalent in the disordered domains. The lateral segregation in complex lipid mixtures was not dramatically affected by the headgroup structure in the monounsaturated lipids, and instead was dominantly affected by the acyl chain saturation/unsaturation. To gain further understanding of lateral segregation in biological membranes, chain position and degree of unsaturation and its effect on headgroup, domain formation, thermostability, and SM-cholesterol interaction should be elucidated.

SUPPORTING MATERIAL

Supporting Materials and Methods, seven figures, and three tables are available at http://www.biophysj.org/biophysj/supplemental/S0006-3495(16)30038-8.

AUTHOR CONTRIBUTIONS

T.N., N.M., M.M., and J.P.S. designed research. O.E., T.Y., and V.H. performed research. All authors analyzed data. O.E. and T.N. wrote the article with contributions from all authors.

ACKNOWLEDGMENTS

Financial support was generously provided by the Academy of Finland (to J.P.S.), the Sigrid Juselius Foundation (to J.P.S.), and the ISB doctoral network at Åbo Akademi (to O.E.). M.M. and N.M. are grateful to the ERATO "Lipid Active Structure Project" from the Japan Science and Technology Agency (to J.S.T.) and to Grant-In-Aids for Scientific Research (A) (No. 25242073) from MEXT, Japan. T.Y. was partly supported by the 'International Joint Research Promotion Program' at Osaka University.

SUPPORTING CITATIONS

References (64–72) appear in the Supporting Material.

REFERENCES

1. van Meer, G., D. R. Voelker, and G. W. Feigenson. 2008. Membrane lipids: where they are and how they behave. *Nat. Rev. Mol. Cell Biol.* 9:112–124.
2. Brügger, B. 2014. Lipidomics: analysis of the lipid composition of cells and subcellular organelles by electrospray ionization mass spectrometry. *Annu. Rev. Biochem.* 83:79–98.
3. Lingwood, D., H. J. Kaiser, …, K. Simons. 2009. Lipid rafts as functional heterogeneity in cell membranes. *Biochem. Soc. Trans.* 37:955–960.
4. Bartels, T., R. S. Lankalapalli, …, M. F. Brown. 2008. Raftlike mixtures of sphingomyelin and cholesterol investigated by solid-state 2H NMR spectroscopy. *J. Am. Chem. Soc.* 130:14521–14532.
5. Ionova, I. V., V. A. Livshits, and D. Marsh. 2012. Phase diagram of ternary cholesterol/palmitoylsphingomyelin/palmitoyloleoyl-phosphatidylcholine mixtures: spin-label EPR study of lipid-raft formation. *Biophys. J.* 102:1856–1865.
6. Op den Kamp, J. A. 1979. Lipid asymmetry in membranes. *Annu. Rev. Biochem.* 48:47–71.

7. Mondal, M., B. Mesmin, …, F. R. Maxfield. 2009. Sterols are mainly in the cytoplasmic leaflet of the plasma membrane and the endocytic recycling compartment in CHO cells. *Mol. Biol. Cell.* 20:581–588.
8. Barenholz, Y. 1984. Sphingomyelin-lecithin balance in membranes: composition, structure, and function relationships. *In* Physiology of Membrane Fluidity. M. Shinitzky, editor. CRC Press, Boca Raton, FL, pp. 131–174.
9. Marsh, D. 2009. Cholesterol-induced fluid membrane domains: a compendium of lipid-raft ternary phase diagrams. *Biochim. Biophys. Acta.* 1788:2114–2123.
10. Soni, S. P., D. S. LoCascio, …, S. R. Wassall. 2008. Docosahexaenoic acid enhances segregation of lipids between : 2H-NMR study. *Biophys. J.* 95:203–214.
11. Shaikh, S. R., A. C. Dumaual, …, S. R. Wassall. 2004. Oleic and docosahexaenoic acid differentially phase separate from lipid raft molecules: a comparative NMR, DSC, AFM, and detergent extraction study. *Biophys. J.* 87:1752–1766.
12. McIntosh, T. J., S. A. Simon, …, C. H. Huang. 1992. Structure and cohesive properties of sphingomyelin/cholesterol bilayers. *Biochemistry.* 31:2012–2020.
13. Chachaty, C., D. Rainteau, …, C. Wolf. 2005. Building up of the liquid-ordered phase formed by sphingomyelin and cholesterol. *Biophys. J.* 88:4032–4044.
14. Talbott, C. M., I. Vorobyov, …, M. C. Yappert. 2000. Conformational studies of sphingolipids by NMR spectroscopy. II. Sphingomyelin. *Biochim. Biophys. Acta.* 1467:326–337.
15. Ohvo-Rekilä, H., B. Ramstedt, …, J. P. Slotte. 2002. Cholesterol interactions with phospholipids in membranes. *Prog. Lipid Res.* 41:66–97.
16. Ramstedt, B., and J. P. Slotte. 1999. Interaction of cholesterol with sphingomyelins and acyl-chain-matched phosphatidylcholines: a comparative study of the effect of the chain length. *Biophys. J.* 76:908–915.
17. Yasuda, T., M. Kinoshita, …, N. Matsumori. 2014. Detailed comparison of deuterium quadrupole profiles between sphingomyelin and phosphatidylcholine bilayers. *Biophys. J.* 106:631–638.
18. Peter Slotte, J. 2013. Molecular properties of various structurally defined sphingomyelins – correlation of structure with function. *Prog. Lipid Res.* 52:206–219.
19. Björkbom, A., T. Róg, …, J. P. Slotte. 2010. Effect of sphingomyelin headgroup size on molecular properties and interactions with cholesterol. *Biophys. J.* 99:3300–3308.
20. Slotte, J. P., M. Jungner, …, R. Bittman. 1994. Effect of sterol side-chain structure on sterol-phosphatidylcholine interactions in monolayers and small unilamellar vesicles. *Biochim. Biophys. Acta.* 1190:435–443.
21. Xu, X., R. Bittman, …, E. London. 2001. Effect of the structure of natural sterols and sphingolipids on the formation of ordered sphingolipid/sterol domains (rafts). Comparison of cholesterol to plant, fungal, and disease-associated sterols and comparison of sphingomyelin, cerebrosides, and ceramide. *J. Biol. Chem.* 276:33540–33546.
22. Meyer, T., D. J. Baek, …, H. A. Scheidt. 2014. Membrane properties of cholesterol analogs with an unbranched aliphatic side chain. *Chem. Phys. Lipids.* 184:1–6.
23. Scheidt, H. A., T. Meyer, …, D. Huster. 2013. Cholesterol's aliphatic side chain modulates membrane properties. *Angew. Chem. Int. Ed. Engl.* 52:12848–12851.
24. Huang, J., and G. W. Feigenson. 1999. A microscopic interaction model of maximum solubility of cholesterol in lipid bilayers. *Biophys. J.* 76:2142–2157.
25. Huang, J., J. T. Buboltz, and G. W. Feigenson. 1999. Maximum solubility of cholesterol in phosphatidylcholine and phosphatidylethanolamine bilayers. *Biochim. Biophys. Acta.* 1417:89–100.
26. Lönnfors, M., J. P. Doux, …, J. P. Slotte. 2011. Sterols have higher affinity for sphingomyelin than for phosphatidylcholine bilayers even at equal acyl-chain order. *Biophys. J.* 100:2633–2641.
27. Niu, S. L., and B. J. Litman. 2002. Determination of membrane cholesterol partition coefficient using a lipid vesicle-cyclodextrin binary system: effect of phospholipid acyl chain unsaturation and headgroup composition. *Biophys. J.* 83:3408–3415.
28. Elson, E. L., E. Fried, …, G. M. Genin. 2010. Phase separation in biological membranes: integration of theory and experiment. *Annu. Rev. Biophys.* 39:207–226.
29. Veatch, S. L., and S. L. Keller. 2005. Seeing spots: complex phase behavior in simple membranes. *Biochim. Biophys. Acta.* 1746: 172–185.
30. Sezgin, E., and P. Schwille. 2011. Fluorescence techniques to study lipid dynamics. *Cold Spring Harb. Perspect. Biol.* 3:a009803.
31. Klymchenko, A. S., and R. Kreder. 2014. Fluorescent probes for lipid rafts: from model membranes to living cells. *Chem. Biol.* 21:97–113.
32. Sklar, L. A., B. S. Hudson, and R. D. Simoni. 1977. Conjugated polyene fatty acids as fluorescent probes: synthetic phospholipid membrane studies. *Biochemistry.* 16:819–828.
33. Sklar, L. A., G. P. Miljanich, and E. A. Dratz. 1979. Phospholipid lateral phase separation and the partition of *cis*-parinaric acid and *trans*-parinaric acid among aqueous, solid lipid, and fluid lipid phases. *Biochemistry.* 18:1707–1716.
34. Silva, L., R. F. de Almeida, …, M. Prieto. 2006. Ceramide-platform formation and -induced biophysical changes in a fluid phospholipid membrane. *Mol. Membr. Biol.* 23:137–148.
35. Engberg, O., H. Nurmi, …, J. P. Slotte. 2015. Effects of cholesterol and saturated sphingolipids on acyl chain order in 1-palmitoyl-2-oleoyl-*sn*-glycero-3-phosphocholine bilayers–a comparative study with phase-selective fluorophores. *Langmuir.* 31:4255–4263.
36. Matsumori, N., T. Yasuda, …, M. Murata. 2012. Comprehensive molecular motion capture for sphingomyelin by site-specific deuterium labeling. *Biochemistry.* 51:8363–8370.
37. Seelig, A., and J. Seelig. 1974. The dynamic structure of fatty acyl chains in a phospholipid bilayer measured by deuterium magnetic resonance. *Biochemistry.* 13:4839–4845.
38. Seelig, J. 1977. Deuterium magnetic resonance: theory and application to lipid membranes. *Q. Rev. Biophys.* 10:353–418.
39. Bloom, M., and J. Thewalt. 1994. Spectroscopic determination of lipid dynamics in membranes. *Chem. Phys. Lipids.* 73:27–38.
40. Björkqvist, Y. J., S. Nybond, …, B. Ramstedt. 2008. *N*-palmitoyl-sulfatide participates in lateral domain formation in complex lipid bilayers. *Biochim. Biophys. Acta.* 1778:954–962.
41. Nyholm, T. K., D. Lindroos, …, J. P. Slotte. 2011. Construction of a DOPC/PSM/cholesterol phase diagram based on the fluorescence properties of *trans*-parinaric acid. *Langmuir.* 27:8339–8350.
42. Yasuda, T., H. Tsuchikawa, …, N. Matsumori. 2015. Deuterium NMR of raft model membranes reveals domain-specific order profiles and compositional distribution. *Biophys. J.* 108:2502–2506.
43. Huster, D., K. Arnold, and K. Gawrisch. 1998. Influence of docosahexaenoic acid and cholesterol on lateral lipid organization in phospholipid mixtures. *Biochemistry.* 37:17299–17308.
44. Sankaram, M. B., and T. E. Thompson. 1990. Modulation of phospholipid acyl chain order by cholesterol. A solid-state 2H nuclear magnetic resonance study. *Biochemistry.* 29:10676–10684.
45. Bunge, A., P. Müller, …, D. Huster. 2008. Characterization of the ternary mixture of sphingomyelin, POPC, and cholesterol: support for an inhomogeneous lipid distribution at high temperatures. *Biophys. J.* 94:2680–2690.
46. Shaikh, S. R., D. S. Locascio, …, W. Stillwell. 2009. Oleic- and docosahexaenoic acid-containing phosphatidylethanolamines differentially phase separate from sphingomyelin. *Biochim. Biophys. Acta.* 1788:2421–2426.
47. Ekman, P., T. Maula, …, J. P. Slotte. 2015. Formation of an ordered phase by ceramides and diacylglycerols in a fluid phosphatidylcholine bilayer–correlation with structure and hydrogen bonding capacity. *Biochim. Biophys. Acta.* 1848 (10 Pt A):2111–2117.

48. Alanko, S. M., K. K. Halling, …, B. Ramstedt. 2005. Displacement of sterols from sterol/sphingomyelin domains in fluid bilayer membranes by competing molecules. *Biochim. Biophys. Acta.* 1715:111–121.

49. Hsueh, Y. W., R. Giles, …, J. Thewalt. 2002. The effect of ceramide on phosphatidylcholine membranes: a deuterium NMR study. *Biophys. J.* 82:3089–3095.

50. Davis, J. H., J. J. Clair, and J. Juhasz. 2009. Phase equilibria in DOPC/DPPC-d62/cholesterol mixtures. *Biophys. J.* 96:521–539.

51. Shaikh, S. R., J. J. Kinnun, …, S. R. Wassall. 2015. How polyunsaturated fatty acids modify molecular organization in membranes: insight from NMR studies of model systems. *Biochim. Biophys. Acta.* 1848 (1 Pt B):211–219.

52. de Almeida, R. F., A. Fedorov, and M. Prieto. 2003. Sphingomyelin/phosphatidylcholine/cholesterol phase diagram: boundaries and composition of lipid rafts. *Biophys. J.* 85:2406–2416.

53. Petruzielo, R. S., F. A. Heberle, …, G. W. Feigenson. 2013. Phase behavior and domain size in sphingomyelin-containing lipid bilayers. *Biochim. Biophys. Acta.* 1828:1302–1313.

54. Sodt, A. J., R. W. Pastor, and E. Lyman. 2015. Hexagonal substructure and hydrogen bonding in liquid-ordered phases containing palmitoyl sphingomyelin. *Biophys. J.* 109:948–955.

55. Heerklotz, H., and A. Tsamaloukas. 2006. Gradual change or phase transition: characterizing fluid lipid-cholesterol membranes on the basis of thermal volume changes. *Biophys. J.* 91:600–607.

56. Konyakhina, T. M., J. Wu, …, G. W. Feigenson. 2013. Phase diagram of a 4-component lipid mixture: DSPC/DOPC/POPC/chol. *Biochim. Biophys. Acta.* 1828:2204–2214.

57. Wang, T. Y., and J. R. Silvius. 2001. Cholesterol does not induce segregation of liquid-ordered domains in bilayers modeling the inner leaflet of the plasma membrane. *Biophys. J.* 81:2762–2773.

58. Heberle, F. A., and G. W. Feigenson. 2011. Phase separation in lipid membranes. *Cold Spring Harb. Perspect. Biol.* 3:a004630.

59. Paré, C., and M. Lafleur. 1998. Polymorphism of POPE/cholesterol system: a 2H nuclear magnetic resonance and infrared spectroscopic investigation. *Biophys. J.* 74:899–909.

60. Bakht, O., P. Pathak, and E. London. 2007. Effect of the structure of lipids favoring disordered domain formation on the stability of cholesterol-containing ordered domains (lipid rafts): identification of multiple raft-stabilization mechanisms. *Biophys. J.* 93:4307–4318.

61. Sergelius, C., S. Yamaguchi, …, J. P. Slotte. 2013. Cholesterol's interactions with serine phospholipids - a comparison of *N*-palmitoyl ceramide phosphoserine with dipalmitoyl phosphatidylserine. *Biochim. Biophys. Acta.* 1828:785–791.

62. Murate, M., M. Abe, …, T. Kobayashi. 2015. Transbilayer distribution of lipids at nano scale. *J. Cell Sci.* 128:1627–1638.

63. Fadok, V. A., D. L. Bratton, …, P. M. Henson. 1998. The role of phosphatidylserine in recognition of apoptotic cells by phagocytes. *Cell Death Differ.* 5:551–562.

64. Davis, J. H. 1983. The description of membrane lipid conformation, order and dynamics by 2H-NMR. *Biochim. Biophys. Acta.* 737:117–171.

65. Térová, B., J. P. Slotte, and T. K. Nyholm. 2004. Miscibility of acyl-chain defined phosphatidylcholines with *N*-palmitoyl sphingomyelin in bilayer membranes. *Biochim. Biophys. Acta.* 1667:182–189.

66. Rouser, G., S. Fkeischer, and A. Yamamoto. 1970. Two dimensional then layer chromatographic separation of polar lipids and determination of phospholipids by phosphorus analysis of spots. *Lipids.* 5: 494–496.

67. Jungner, M., H. Ohvo, and J. P. Slotte. 1997. Interfacial regulation of bacterial sphingomyelinase activity. *Biochim. Biophys. Acta.* 1344: 230–240.

68. Kuklev, D. V., and W. L. Smith. 2004. Synthesis of four isomers of parinaric acid. *Chem. Phys. Lipids.* 131:215–222.

69. Björkqvist, Y. J., J. Brewer, …, B. Westerlund. 2009. Thermotropic behavior and lateral distribution of very long chain sphingolipids. *Biochim. Biophys. Acta.* 1788:1310–1320.

70. Huang, C., and J. T. Mason. 1986. Structure and properties of mixed-chain phospholipid assemblies. *Biochim. Biophys. Acta.* 864:423–470.

71. McCabe, M. A., and S. R. Wassall. 1997. Rapid deconvolution of NMR powder spectra by weighted fast Fourier transformation. *Solid State Nucl. Magn. Reson.* 10:53–61.

72. Halling, K. K., B. Ramstedt, …, T. K. Nyholm. 2008. Cholesterol interactions with fluid-phase phospholipids: effect on the lateral organization of the bilayer. *Biophys. J.* 95:3861–3871.

Biophysical Journal, Volume *110*

Supplemental Information

Lipid Interactions and Organization in Complex Bilayer Membranes

Oskar Engberg, Tomokazu Yasuda, Victor Hautala, Nobuaki Matsumori, Thomas K.M. Nyholm, Michio Murata, and J. Peter Slotte

Supplemental information: Materials and methods, 7 figures, 3 tables, and 10 references.

Lipid Interactions and Organization in Complex Bilayer Membranes

Oskar Engberg [1#], Tomokazu Yasuda [2,3#], Victor Hautala [1], Nobuaki Matsumori[2,4], Thomas K.M. Nyholm[1], Michio Murata [2,3] and J. Peter Slotte [1]

[1] Biochemistry, Faculty of Science and Engineering, Åbo Akademi University, Tykistökatu 6A, FIN-20520 Turku, Finland
[2] Department of Chemistry, Graduate School of Science, Osaka University, Toyonaka, Osaka, Japan
[3] Japan Science and Technology Agency, ERATO, Lipid Active Structure Project, Toyonaka, Osaka, Japan
[4] Department of Chemistry, Faculty of Science, Kyushu University, Fukuoka, Japan

# equal contribution

MATERIALS AND METHODS

Materials

POPC, POPE, POPS, POPC-d_{31}, POPE-d_{31}, POPS-d_{31}, 1-oleoyl-2-hydroxy-*sn*-glycero-3-phosphocholine (O-lyso-PC), *N*-palmitoyl(d_{31})-D-*erythro*-sphingosylphosphorylcholine (PSM-d_{31}), D-*erythro*-sphingosyl-phosphorylcholine (lyso-SM) and egg sphingomyelin (egg SM) were purchased from Avanti Polar lipids (Alabaster, AL, U.S.A.). Reverse-phase HPLC was used to purify PSM from egg SM as previously described in (1). Cholesterol was purchased from Sigma-Aldrich (St, Louis, MO, U.S.A.). All lipids were dissolved in methanol except cholesterol and POPE which were dissolved in hexane/isopropanol (3:2 by volume) and methanol/hexane/2-propanol (10:3:2 by volume) respectively. All stock solutions were stored at -20 °C and taken to ambient temperature before use. The PL concentrations were determined with an inorganic phosphate assay as described by Rouser and co-workers (2). A surface barostat was used to determine the cholesterol concentration as described in (3). Water used in buffer preparation was purified by reverse osmosis and passage through a Millipore UF Plus water purification system to a final resistivity of 18.2 MΩcm. The solvents used were of spectroscopic grade and other inorganic and organic chemicals used were of the highest available purity.

Synthesis of trans-parinaric acid and its derivatives

tPA was synthesized in house from the methyl ester of α-linolenic acid according to the method reported by Kuklev and Smith (4). tPA was purified by crystallization from hexane at -80°C to yield 99% pure all trans tPA. *N*-tPA-sphingosylphosphorylcholine (tPA-SM) was synthesized by *N*-acylation of lyso-SM with tPA as described previously (5). 1-oleoyl-2-tPA-*sn*-3-glycero-phosphatidylcholine (O-tPA-PC) was synthesized by acylation of 1-18:1/2-OH-lyso-PC as described in (6). The tPA-containing PLs were purified using HPLC with a Discovery C18 column (Supelco, Bellefonte, PA, U.S.A.) using pure methanol as eluent. tPA and tPA derivatives were identified and confirmed pure based on ESI-MS data (Bruker Daltonics, Bremen, Germany), absorbance and fluorescence properties, and analytical HPLC analysis. Fluorophores were stored at −87 °C under argon in GC vials until the fluorophores were

dissolved in argon-purged methanol. Fluorophore concentrations were determined with absorbance using the molar extinction coefficients of 92000 $cm^{-1}M^{-1}$ at 300 nm in methanol for tPA derivatives (7). Dilute stock solutions of fluorophores were stored at −20 °C and used within a week.

^{2}H NMR sample preparation

The binary bilayers contained 14 μmol of either POPC, POPE, or POPS and 7 μmol 9',9'-d_2 -PSM . The ternary bilayers had additional 7 μmol of cholesterol. The complex bilayers contained 7 μmol PSM + 14 μmol POPC + 5.25 μmol each of POPE and POPS. PSM was perdeuterated in the *N*-palmitoyl chain (PSM-d_{31}) and the unsaturated lipids had a perdeuterated palmitoyl chain in the *sn-1* position (POPC-d_{31}, POPE-d_{31}, POPS-d_{31}). The total PL content in complex bilayers was 31.5 μmol with varying cholesterol concentration (0, 10, 18, 25, 31 mol%). The samples were mixed in glass tubes and the solvent evaporated under a constant stream of nitrogen at 40 °C and re-dissolved in 0.5 ml chloroform to give a more homogenous mixing of the lipids before they again were dried under a constant nitrogen flow at 40 °C. This was followed by overnight high vacuum. Multilamellar vesicles (MLV) were prepared by hydrating the dried lipid films with 1 ml of pure water at 65 °C followed by vigorous vortexing. Each suspension was freeze thawed three times followed by lyophilization, rehydration with deuterium depleted water until 50% hydrated (w/w) and freeze-thawed three times. Each sample was transferred to a 5 mm glass tube (Wilmad, Vineland, NJ, U.S.A.) and sealed using epoxy glue.

^{2}H NMR measurements and analysis

^{2}H measurements were recorded on a 300-MHz CMX spectrometer (Chemagnetics, Agilent, Palo Alto, CA, U.S.A.) using a 5-mm ^{2}H static probe (Otsuka Electronics, Osaka, Japan) and a quadrupole echo sequence. The 90° pulse width was 2 μs, the interpulse delay was 30 μs and the repetition rate was 0.5 s. The number of scans was approximately 100 000 and sweep width was 200 kHz. The NMR data were analyzed with TopSpin software (Bruker) and 300 Hz of line broadening was used. The first spectral moment (M_1) was calculated for each ^{2}H spectra using the following equation:

$$M_1 = \frac{\int_{-\infty}^{\infty} |\omega| f(\omega) d\omega}{\int_{-\infty}^{\infty} f(\omega) d\omega} \quad (1)$$

where ω is the frequency with respect to the central Larmor frequency ω_0, $f(\omega)$ is the line shape, and n is the order of the spectral moment (8). The chosen spectra were fast Fourier transform dePaked to enhance the resolution and give spectra similar to a planar membrane of single alignment (9).

Fluorescence experiments

For time resolved fluorescence experiments MLVs were prepared in Tris buffer (50 mM Tris pH 7.4, 140 mM NaCl) to the final PL concentration of 0.1 mM for the binary bilayer and 0.2 mM for the ternary bilayers. Cholesterol was added in a concentration of 31 mol% for the ternary and 47 mol% for the binary bilayers. A maximum of 1 mol% of O-tPA-PC or tPA-SM fluorophores were added to glass tubes. The solvent was evaporated under nitrogen flow at 40 °C. The fully dried lipid films were hydrated in pre-warmed argon purged Tris buffer at 55 °C for 30 min and then vortexed and sonicated at 55 °C for 5 min in a FinnSonic M3 Bath

Sonicator (FinnSonic Oy, Lahti, Finland). The samples were cooled to room temperature before measurements were performed at 20, 25, 30, 40 and 50 °C using a FluoTime 200 instrument (PicoQuant Gmb, Berlin, Germany). The fluorophores were excited with a PLS LED laser with a maximum signal at 298 nm, and the emission was collected at 405 nm. The fluorescence decays were analyzed using FluoFit Pro software (PicoQuant Gmb).

DATA GRAPHS AND TABLES

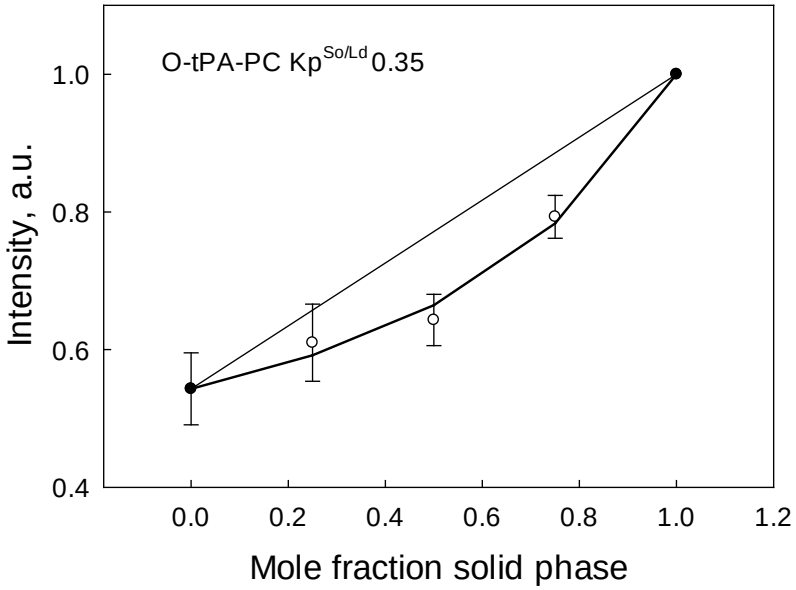

Figure S1. Partitioning of O-tPA-PC between gel and fluid phase at 23°C. The steady-state intensity of O-tPA measured in POPC/PSM bilayers. The lipid compositions was selected based on the binary POPC/PSM phase diagram (10) so that the fraction of gel phase in the samples was increased from 0 to 100. The partition coefficients ($K_p^{So/ld}$) were obtained by fitting the data with equation 1.

$$I = \frac{\mathrm{K}(\varepsilon_g \phi_g K_p X_g + \varepsilon_f \phi_f X_f}{(K_p X_g + X_f)} \quad (1)$$

the suffix *g* indicates results obtained in the gel phase and *f* indicates the fluid phase. *K* is the factor used to normalize the fluorescence intensity values, ε is the molar extinction coefficient, $\phi$is the quantum yield and *X* denotes the fraction of each phase present as determined from the binary phase-diagram. K_p was obtained by fitting the equations to the experimental data. The obtained $K_p^{So/ld}$ value is shown in the figure legends. The simulated data is shown as a line connecting the dots and compared with an ideal 1:1 partitioning. Similar results were obtained with anisotropy and lifetime data (data not shown). n = 5.

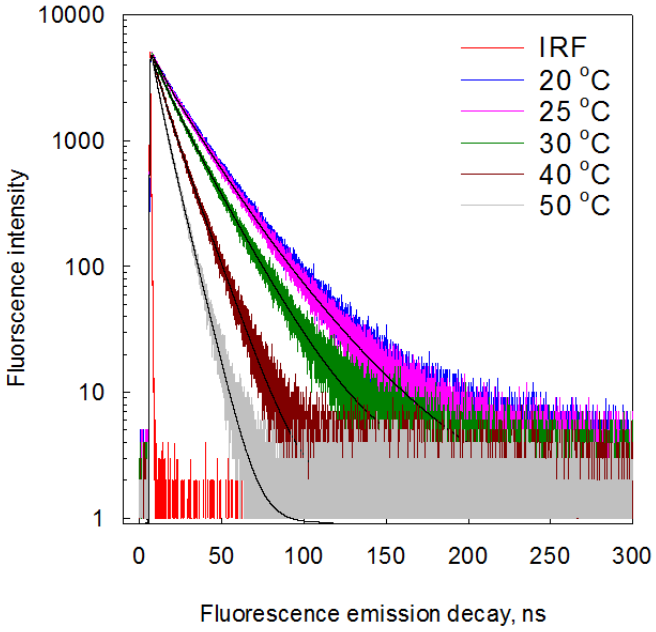

Figure S2. Decays of tPA-SM in POPC/PSM/Chol (34.5: 34.5: 30 mol%) multilamellar vesicles as a function of temperature. IRF= instrument background factor. Note the logarithmic scale.

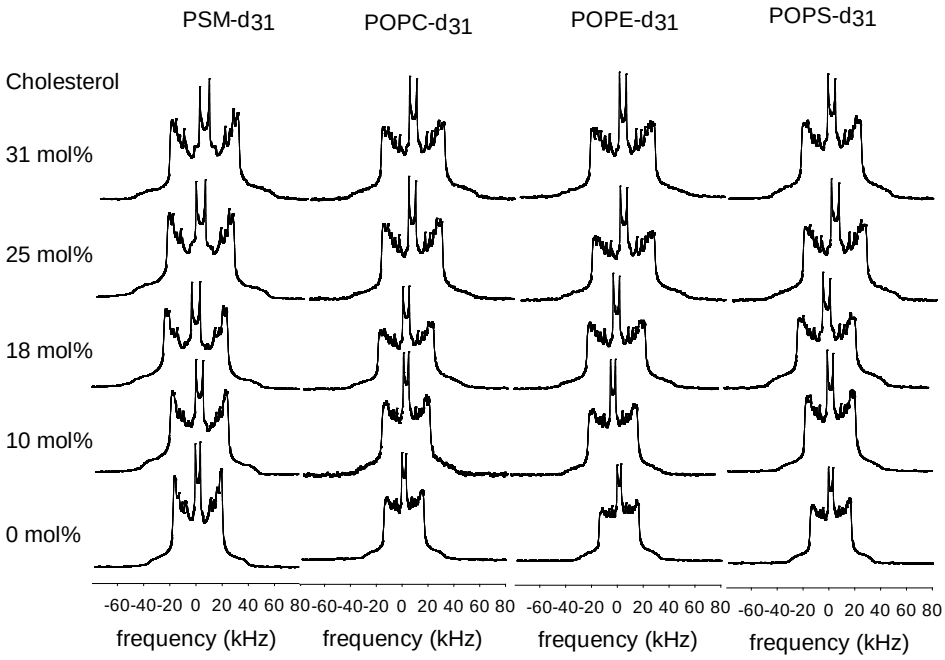

Figure S3. ^{2}H Spectra of complex bilayers at 20 °C as a cholesterol gradient. Multilamellar vesicles were prepared to 50 % hydration and the bilayers contained PSM/POPC/POPE/POPS 22:44:17:17 in the sample without cholesterol.

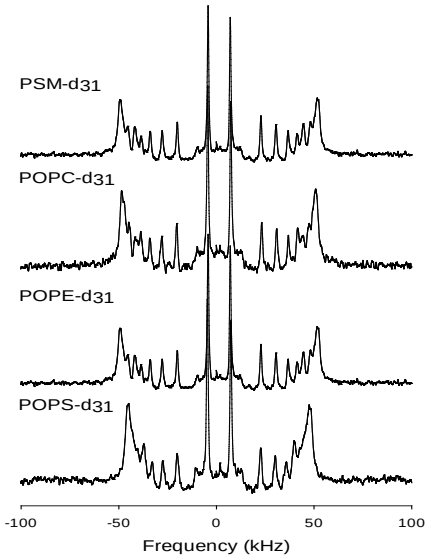

Figure S4. No double Pake peaks were observed in each perdeuterated lipid in the complex bilayers. The spectra were dePaked to show if double Pake peaks are observed. The spectra is at 20 °C at the highest cholesterol concentration (31 mol%) measured but the same results were obtained at all temperatures and cholesterol concentrations. Multilamellar vesicles were prepared to 50 % hydration with the composition PSM/POPC/POPE/POPS 22:44:17:17 + 31 mol% cholesterol.

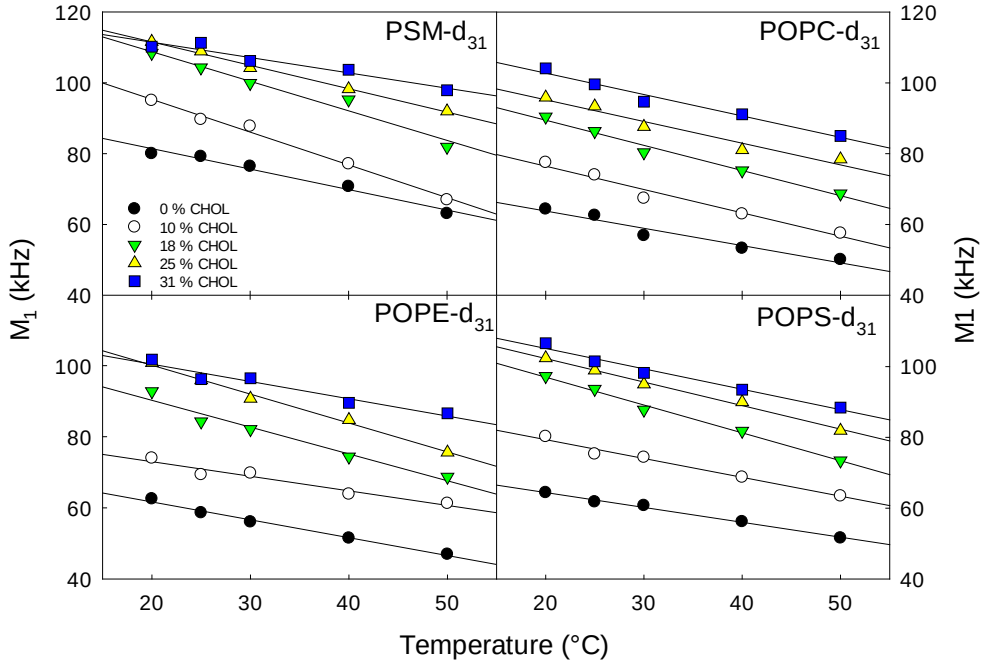

Figure S5. Cholesterol induced ordering of perdeuterated lipids in complex bilayers as a function of temperature. Ordering was measured as the first spectral moment (M_1). The data is shown for each perdeuterated lipid in each panel, as a cholesterol gradient. Multilamellar vesicles were prepared to 50 % hydration with the composition PSM/POPC/POPE/POPS 22:44:17:17 plus addition of 10-31 mol % cholesterol. The lines are only a guide to the eye.

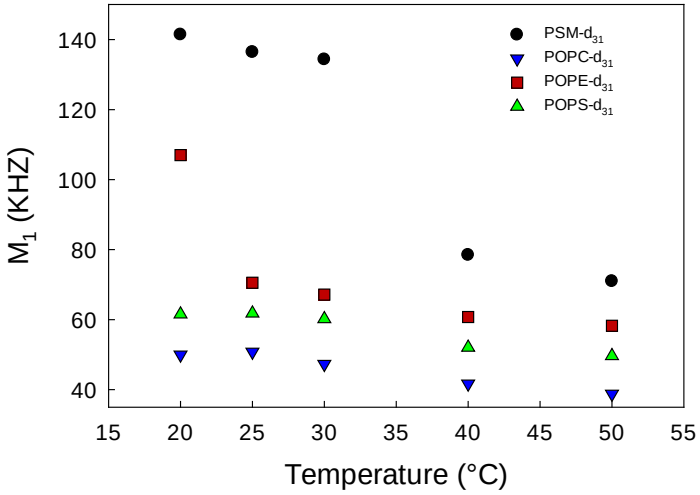

Figure S6. Pure perdeuterated lipid as a function of temperature. Ordering was measured as the first spectral moment (M_1). Multilamellar vesicles were prepared to 50 % hydration.

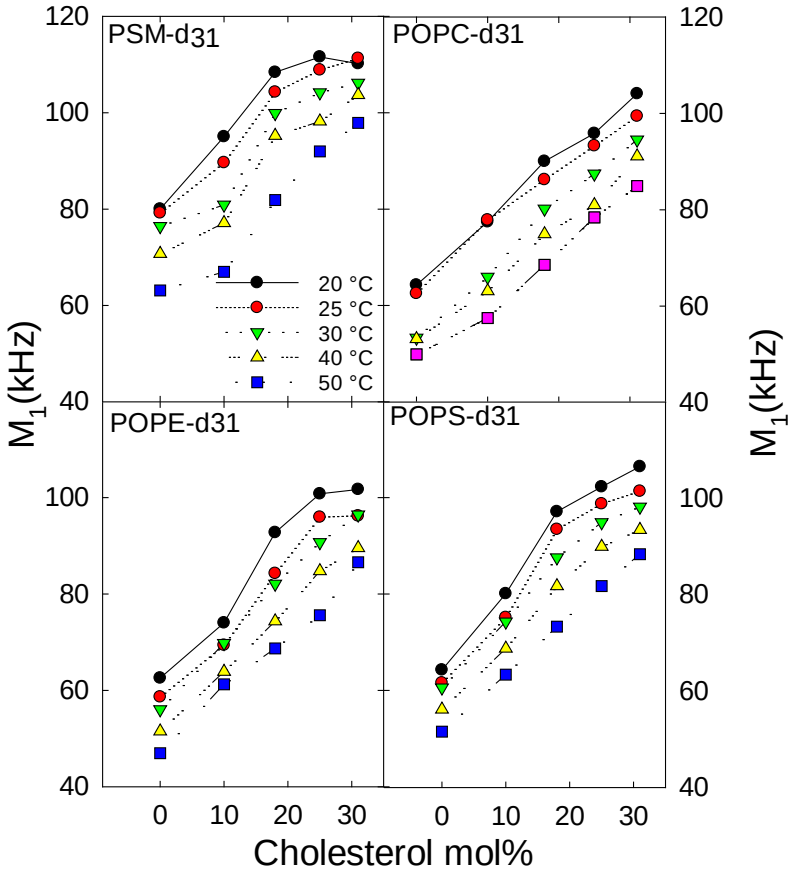

Figure S7. Acyl chain order of perdeuterated lipids in complex bilayers at different temperatures as a function of cholesterol concentration. Ordering was measured as the first spectral moment (M_1).Panel A) PSM-d_{31} B) POPC-d_{31}, C) POPE-d_{31} D) POPS-d_{31}. Multilamellar vesicles were prepared to 50 % hydration.

Table S1: Comparison of time resolved fluorescence decays reported by 1 mol% of O-tPA-PC and tPA-SM in identical bilayers at 20 °C.

Probe tests

Sample	Probe	I τAV			τ1			τ 2			τ 3			α1			α2			α3		
PSM	**tPA-SM**	**50.1**	±	*3.12*	**67.0**	±	*8.10*	**43.6**	±	*5.37*	**3.4**	±	*2.25*	**0.21**	±	*0.07*	**0.65**	±	*0.02*	**0.13**	±	*0.05*
PSM	**O-tPA-PC**	**40.2**	±	*0.37*	**51.3**	±	*2.14*	**23.0**	±	*0.42*	**3.2**	±	*0.01*	**0.26**	±	*0.03*	**0.22**	±	*0.03*	**0.52**	±	*0.00*
POPC	**tPA-SM**	**7.0**	±	*0.55*				**7.5**	±	*0.54*	**3.2**	±	*0.04*				**0.73**	±	*0.02*	**0.27**	±	*0.02*
POPC	**O-tPA-PC**	**5.5**	±	*0.33*				**6.3**	±	*0.27*	**2.9**	±	*0.49*				**0.59**	±	*0.04*	**0.41**	±	*0.04*
PSM/Chol	**tPA-SM**	**29.6**	±	*0.25*	**45.9**	±	*5.37*	**24.7**	±	*2.50*	**6.2**	±	*2.54*	**0.16**	±	*0.08*	**0.70**	±	*0.04*	**0.14**	±	*0.04*
PSM/Chol	**O-tPA-PC**	**19.5**	±	*0.85*	**39.2**	±	*1.11*	**18.8**	±	*0.61*	**6.3**	±	*1.25*	**0.05**	±	*0.02*	**0.63**	±	*0.03*	**0.32**	±	*0.01*
POPC/Chol	**tPA-SM**	**17.8**	±	*0.97*				**19.3**	±	*0.56*	**8.2**	±	*2.59*				**0.73**	±	*0.08*	**0.27**	±	*0.08*
POPC/Chol	**O-tPA-PC**	**13.1**	±	*0.27*				**14.3**	±	*0.73*	**6.5**	±	*3.10*				**0.69**	±	*0.08*	**0.31**	±	*0.08*

Multilamellar vesicles were prepared with 1 mol % probe to a composition of pure phospholipid or phospholipid: cholesterol (53; 47 mol%) in the binary bilayers and measured at 20 °C. I τAV, intensity weighted average lifetime (ns); α, fractional amplitudes. All samples were measured at 20 °C.

Table S2: Detection of membrane order by time resolved fluorescence decays of domain selective probes in binary and ternary multi-lamellar vesicles as function of temperature.

POPC O-tPA-PC

temp	I τAV			τ1			τ 2			α1			α2		
20	**5.7**	±	*0.07*	**7.1**	±	*0.22*	**4.1**	±	*0.09*	**0.38**	±	*0.01*	**0.62**	±	*0.01*
25	**4.7**	±	*0.03*	**6.5**	±	*0.07*	**3.7**	±	*0.18*	**0.25**	±	*0.04*	**0.75**	±	*0.04*
30	**3.9**	±	*0.01*	**6.3**	±	*0.28*	**3.3**	±	*0.15*	**0.13**	±	*0.04*	**0.87**	±	*0.04*
40	**3.0**	±	*0.05*	**6.0**	±	*0.31*	**2.6**	±	*0.02*	**0.05**	±	*0.02*	**0.95**	±	*0.02*
50	**2.3**	±	*0.02*	**4.9**	±	*0.03*	**2.0**	±	*0.02*	**0.06**	±	*0.01*	**0.94**	±	*0.01*

POPC/Chol O-tPA-PC

temp	I τAV			τ1			τ 2			α1			α2		
20	**13.2**	±	*0.08*	**14.8**	±	*0.02*	**8.7**	±	*0.69*	**0.63**	±	*0.04*	**0.37**	±	*0.04*
25	**10.8**	±	*0.28*	**11.9**	±	*0.23*	**5.6**	±	*0.28*	**0.71**	±	*0.02*	**0.29**	±	*0.02*
30	**9.0**	±	*0.09*	**10.1**	±	*0.12*	**5.5**	±	*0.18*	**0.64**	±	*0.01*	**0.36**	±	*0.01*
40	**6.5**	±	*0.07*	**8.4**	±	*0.24*	**5.6**	±	*0.16*	**0.24**	±	*0.07*	**0.76**	±	*0.07*
50	**4.7**	±	*0.15*	**7.1**	±	*0.77*	**3.9**	±	*0.31*	**0.15**	±	*0.06*	**0.85**	±	*0.06*

POPC/PSM/Chol O-tPA-PC

temp	I τAV			τ1			τ 2			α1			α2		
20	**16.0**	±	*0.85*	**22.6**	±	*2.93*	**11.0**	±	*3.06*	**0.28**	±	*0.15*	**0.72**	±	*0.15*
25	**12.9**	±	*0.19*	**16.4**	±	*0.62*	**7.3**	±	*0.46*	**0.42**	±	*0.04*	**0.58**	±	*0.04*
30	**10.0**	±	*0.13*	**12.5**	±	*0.45*	**5.7**	±	*0.24*	**0.43**	±	*0.04*	**0.57**	±	*0.04*
40	**6.4**	±	*0.50*	**8.3**	±	*0.33*	**4.1**	±	*0.36*	**0.38**	±	*0.16*	**0.62**	±	*0.16*
50	**4.5**	±	*0.06*	**6.0**	±	*0.16*	**3.1**	±	*0.14*	**0.33**	±	*0.02*	**0.67**	±	*0.02*

PSM tPA-SM

temp	τAV			τ1			τ 2			τ 3			α1			α2			α3		
20	**46.9**	±	*0.05*	**53.3**	±	*0.04*	**29.3**	±	*0.03*				**0.60**	±	*0.01*	**0.40**	±	*0.01*			
25	**42.3**	±	*0.01*	**49.7**	±	*0.35*	**28.0**	±	*0.58*				**0.52**	±	*0.02*	**0.48**	±	*0.02*			
30	**37.1**	±	*0.07*	**45.0**	±	*0.93*	**25.5**	±	*0.95*				**0.45**	±	*0.05*	**0.55**	±	*0.05*			
40	**25.1**	±	*0.24*	**42.6**	±	*16.4*	**19.7**	±	*6.61*	**6.2**			**0.24**	±	*0.29*	**0.61**	±	*0.07*	**0.15**	±	*0.05*
50	**3.8**	±	*0.19*				**5.4**	±	*0.50*	**3.0**	±	*0.50*				**0.22**	±	*0.09*	**0.78**	±	*0.09*

PSM/Chol tPA-SM

temp	τAV			τ1			τ 2			τ 3			α1			α2			α3		
20	**26.5**	±	*0.68*	**41.1**	±	*1.50*	**21.3**	±	*0.69*	**3.6**	±	*0.78*	**0.15**	±	*0.05*	**0.61**	±	*0.12*	**0.23**	±	*0.16*
25	**23.5**	±	*0.29*	**39.3**	±	*2.61*	**20.5**	±	*0.93*	**4.6**	±	*2.37*	**0.10**	±	*0.03*	**0.66**	±	*0.04*	**0.24**	±	*0.04*
30	**20.0**	±	*0.42*	**36.9**	±	*3.89*	**18.5**	±	*0.95*	**5.3**	±	*2.14*	**0.07**	±	*0.04*	**0.69**	±	*0.03*	**0.24**	±	*0.04*
40	**14.5**	±	*0.37*	**27.5**	±	*1.83*	**14.3**	±	*0.35*	**3.5**	±	*0.44*	**0.03**	±	*0.01*	**0.75**	±	*0.01*	**0.22**	±	*0.01*
50	**10.2**	±	*0.04*				**11.0**	±	*0.08*	**4.7**	±	*0.01*				**0.74**	±	*0.01*	**0.26**	±	*0.01*

POPC/PSM/Chol tPA-SM

temp	τAV			τ1			τ 2			τ 3			α1			α2			α3		
20	**27.1**	±	*0.96*	**44.1**	±	*3.10*	**23.5**	±	*0.90*	**5.3**	±	*2.58*	**0.11**	±	*0.03*	**0.77**	±	*0.05*	**0.12**	±	*0.06*
25	**22.2**	±	*0.68*	**35.3**	±	*3.02*	**18.8**	±	*1.55*	**4.1**	±	*1.97*	**0.13**	±	*0.05*	**0.73**	±	*0.09*	**0.14**	±	*0.05*
30	**17.6**	±	*0.37*	**34.7**	±	*2.83*	**17.0**	±	*0.41*	**5.9**	±	*0.58*	**0.04**	±	*0.01*	**0.77**	±	*0.01*	**0.20**	±	*0.02*
40	**11.0**	±	*0.26*				**12.2**	±	*0.20*	**5.7**	±	*0.23*				**0.67**	±	*0.06*	**0.33**	±	*0.06*
50	**7.2**	±	*0.03*				**8.1**	±	*0.03*	**3.9**	±	*0.09*				**0.66**	±	*0.01*	**0.34**	±	*0.01*

POPE O-tPA-PC

temp	τAV			τ1			τ 2			α1			α2		
20	**25.9**	±	*0.36*	**31.8**	±	*0.10*	**8.9**	±	*2.55*	**0.44**	±	*0.01*	**0.56**	±	*0.01*
25	**8.1**	±	*1.29*	**16.1**	±	*7.97*	**6.1**	±	*1.23*	**0.14**	±	*0.13*	**0.86**	±	*0.13*
30	**5.4**	±	*0.24*	**6.3**	±	*0.14*	**2.6**	±	*0.27*	**0.59**	±	*0.04*	**0.41**	±	*0.04*
40	**4.0**	±	*0.19*	**5.6**	±	*1.01*	**2.2**	±	*0.54*	**0.32**	±	*0.12*	**0.68**	±	*0.12*
50	**3.3**	±	*0.66*	**5.5**	±	*0.26*	**1.8**	±	*0.65*	**0.17**	±	*0.11*	**0.83**	±	*0.11*

POPE/Chol O-tPA-PC

temp	τAV			τ1			τ 2			α1			α2		
20	**12.1**	±	*0.43*	**13.8**	±	*0.30*	**6.1**	±	*1.06*	**0.61**	±	*0.13*	**0.39**	±	*0.13*
25	**10.6**	±	*0.46*	**11.6**	±	*0.07*	**4.6**	±	*0.65*	**0.71**	±	*0.11*	**0.29**	±	*0.11*
30	**8.7**	±	*0.31*	**9.6**	±	*0.03*	**3.1**	±	*0.52*	**0.65**	±	*0.11*	**0.35**	±	*0.11*
40	**6.2**	±	*1.28*	**7.2**	±	*0.81*	**2.7**	±	*1.89*	**0.52**	±	*0.23*	**0.48**	±	*0.23*
50	**4.6**	±	*0.40*	**5.6**	±	*0.23*	**2.5**	±	*1.15*	**0.46**	±	*0.06*	**0.54**	±	*0.06*

POPE/PSM/Chol O-tPA-PC

temp	τAV			τ1			τ 2			α1			α2		
20	**18.6**	±	*0.31*	**27.8**	±	*0.16*	**15.8**	±	*0.19*	**0.15**	±	*0.01*	**0.85**	±	*0.01*
25	**15.0**	±	*0.40*	**20.1**	±	*2.77*	**11.1**	±	*3.43*	**0.30**	±	*0.23*	**0.70**	±	*0.23*
30	**11.9**	±	*0.08*	**13.4**	±	*0.05*	**6.2**	±	*0.10*	**0.63**	±	*0.02*	**0.37**	±	*0.02*
40	**7.8**	±	*0.03*	**8.7**	±	*0.09*	**3.9**	±	*0.14*	**0.67**	±	*0.04*	**0.33**	±	*0.04*
50	**5.2**	±	*0.04*	**6.3**	±	*0.04*	**3.5**	±	*0.01*	**0.46**	±	*0.01*	**0.54**	±	*0.01*

POPE/PSM/Chol tPA-SM

temp	I τAV			τ1			τ 2			τ 3			α1			α2			α3		
20	**28.7**	±	*1.90*	**43.7**	±	*0.53*	**24.3**	±	*0.39*	**6.7**	±	*1.75*	**0.14**	±	*0.05*	**0.74**	±	*0.08*	**0.17**	±	*0.05*
25	**23.9**	±	*0.97*	**39.6**	±	*1.87*	**21.4**	±	*0.46*	**5.7**	±	*0.18*	**0.09**	±	*0.03*	**0.80**	±	*0.08*	**0.16**	±	*0.10*
30	**19.1**	±	*0.49*	**25.4**	±	*1.75*	**15.5**	±	*0.93*	**3.8**	±	*0.60*	**0.26**	±	*0.07*	**0.62**	±	*0.07*	**0.12**	±	*0.05*
40	**12.4**	±	*0.41*				**13.4**	±	*0.17*	**5.0**	±	*1.89*				**0.73**	±	*0.11*	**0.27**	±	*0.11*
50	**8.3**	±	*0.09*				**9.0**	±	*0.25*	**4.4**	±	*1.16*				**0.72**	±	*0.06*	**0.28**	±	*0.06*

POPS O-tPA-PC

temp	I τAV			τ1			τ 2			α1			α2		
20	**6.1**	±	*0.03*	**7.6**	±	*0.27*	**3.7**	±	*0.16*	**0.45**	±	*0.07*	**0.55**	±	*0.07*
25	**5.0**	±	*0.06*	**7.0**	±	*0.69*	**3.7**	±	*0.19*	**0.27**	±	*0.09*	**0.73**	±	*0.09*
30	**4.2**	±	*0.07*	**7.6**	±	*0.42*	**3.6**	±	*0.09*	**0.08**	±	*0.01*	**0.92**	±	*0.01*
40	**3.1**	±	*0.01*	**7.4**	±	*1.08*	**2.7**	±	*0.01*	**0.03**	±	*0.01*	**0.97**	±	*0.01*
50	**2.4**	±	*0.01*	**6.7**	±	*0.99*	**2.1**	±	*0.01*	**0.03**	±	*0.01*	**0.97**	±	*0.01*

POPS/Chol O-tPA-PC

temp	I τAV			τ1			τ 2			α1			α2		
20	**10.4**	±	*0.36*	**12.3**	±	*0.03*	**5.2**	±	*0.08*	**0.54**	±	*0.06*	**0.46**	±	*0.06*
25	**9.0**	±	*0.16*	**10.5**	±	*0.02*	**4.5**	±	*0.14*	**0.57**	±	*0.03*	**0.43**	±	*0.03*
30	**7.5**	±	*0.04*	**9.1**	±	*0.01*	**4.3**	±	*0.01*	**0.50**	±	*0.01*	**0.50**	±	*0.01*
40	**5.6**	±	*0.08*	**7.1**	±	*0.11*	**3.6**	±	*0.27*	**0.39**	±	*0.06*	**0.61**	±	*0.06*
50	**4.3**	±	*0.01*	**5.8**	±	*0.08*	**2.9**	±	*0.02*	**0.33**	±	*0.01*	**0.67**	±	*0.01*

POPS/PSM/Chol O-tPA-PC

temp	I τAV			τ1			τ 2			α1			α2		
20	**17.7**	±	*0.09*	**24.2**	±	*0.36*	**8.9**	±	*0.14*	**0.33**	±	*0.02*	**0.67**	±	*0.02*
25	**13.8**	±	*1.04*	**20.3**	±	*0.89*	**8.7**	±	*1.81*	**0.25**	±	*0.13*	**0.75**	±	*0.13*
30	**11.6**	±	*0.21*	**15.5**	±	*0.04*	**6.2**	±	*0.04*	**0.35**	±	*0.02*	**0.65**	±	*0.02*
40	**8.1**	±	*0.07*	**10.0**	±	*0.25*	**4.0**	±	*0.36*	**0.46**	±	*0.02*	**0.54**	±	*0.02*
50	**5.6**	±	*0.21*	**7.1**	±	*0.11*	**3.0**	±	*0.01*	**0.43**	±	*0.03*	**0.57**	±	*0.03*

POPS/PSM/Chol tPA-SM

temp	I τAV			τ1			τ 2			τ 3			α1			α2			α3		
20	**30.8**	±	*1.18*	**51.5**	±	*4.50*	**27.1**	±	*1.49*	**9.4**	±	*1.55*	**0.11**	±	*0.04*	**0.63**	±	*0.02*	**0.26**	±	*0.07*
25	**26.0**	±	*0.77*	**48.0**	±	*5.24*	**24.2**	±	*0.98*	**8.6**	±	*0.76*	**0.07**	±	*0.03*	**0.63**	±	*0.04*	**0.29**	±	*0.06*
30	**21.2**	±	*0.59*	**42.8**	±	*0.63*	**20.7**	±	*0.53*	**7.2**	±	*1.06*	**0.04**	±	*0.01*	**0.63**	±	*0.03*	**0.32**	±	*0.02*
40	**13.9**	±	*0.23*				**16.8**	±	*0.27*	**7.0**	±	*0.57*				**0.49**	±	*0.01*	**0.51**	±	*0.01*
50	**9.7**	±	*0.13*				**10.8**	±	*0.03*	**3.8**	±	*0.42*				**0.65**	±	*0.02*	**0.35**	±	*0.02*

I τAVG, intensity weighted average lifetime (ns); α, fractional amplitudes. 1 mol% of the fluorescent probes tPA-SM (partitions to ordered domains) or O-tPA-PC (partition to disordered domains) were included in the bilayer.

Table S3: Detection of membrane order by time resolved fluorescence decays of phase selective probes in complex five-component bilayers as function of temperature.

Complex bilayer O-tPA-PC

temp	I τAV	τ1	τ 2	α1	α2
20	**7.0** ± *0.04*	**9.1** ± *0.70*	**3.5** ± *1.04*	**0.39** ± *0.09*	**0.61** ± *0.09*
25	**5.6** ± *0.07*	**7.4** ± *0.34*	**3.2** ± *0.85*	**0.35** ± *0.09*	**0.65** ± *0.09*
30	**4.7** ± *0.16*	**6.7** ± *0.34*	**3.0** ± *0.80*	**0.27** ± *0.12*	**0.73** ± *0.12*
40	**3.6** ± *0.49*	**7.1** ± *0.28*	**2.6** ± *0.33*	**0.09** ± *0.06*	**0.91** ± *0.06*
50	**3.1** ± *0.92*	**7.2** ± *0.08*	**2.0** ± *0.22*	**0.07** ± *0.07*	**0.93** ± *0.07*

Complex bilayer/Chol O-tPA-PC

temp	I τAV	τ1	τ 2	α1	α2
20	**13.9** ± *0.30*	**16.0** ± *0.68*	**5.9** ± *2.13*	**0.57** ± *0.02*	**0.43** ± *0.02*
25	**11.3** ± *0.41*	**12.6** ± *0.35*	**4.1** ± *1.02*	**0.64** ± *0.04*	**0.36** ± *0.04*
30	**9.0** ± *0.20*	**10.1** ± *0.21*	**3.8** ± *1.02*	**0.71** ± *0.14*	**0.29** ± *0.14*
40	**6.0** ± *0.04*	**7.2** ± *0.36*	**3.3** ± *0.94*	**0.51** ± *0.09*	**0.49** ± *0.09*
50	**4.3** ± *0.09*	**5.8** ± *0.71*	**2.8** ± *0.80*	**0.32** ± *0.21*	**0.68** ± *0.21*

Complex bilayer tPA-SM

temp	I τAV	τ1	τ 2	τ 3	α1	α2	α3
20	**13.0** ± *1.60*	**25.0** ± *8.42*	**11.2** ± *2.21*	**3.9** ± *1.53*	**0.09** ± *0.06*	**0.65** ± *0.03*	**0.25** ± *0.10*
25	**8.7** ± *0.51*	**14.1** ± *2.90*	**9.8** ± *0.34*	**4.7** ± *0.01*	**0.03** ± *0.01*	**0.54** ± *0.05*	**0.43** ± *0.04*
30	**6.5** ± *0.18*		**7.4** ± *0.21*	**3.5** ± *0.05*		**0.59** ± *0.00*	**0.41** ± *0.00*
40	**4.2** ± *0.05*		**5.6** ± *0.42*	**3.1** ± *0.31*		**0.31** ± *0.10*	**0.69** ± *0.10*
50	**3.0** ± *0.05*		**5.3** ± *0.77*	**2.5** ± *0.18*		**0.10** ± *0.06*	**0.90** ± *0.06*

Complex bilayer/Chol tPA-SM

temp	I τAV	τ1	τ 2	τ 3	α1	α2	α3
20	**21.7** ± *1.12*	**26.9** ± *1.65*	**13.2** ± *4.35*		**0.43** ± *0.05*	**0.57** ± *0.05*	
25	**17.8** ± *0.38*	**25.4** ± *3.06*	**15.8** ± *1.09*	**3.34** ± *0.94*	**0.17** ± *0.09*	**0.66** ± *0.18*	**0.18** ± *0.09*
30	**14.2** ± *0.08*		**15.4** ± *0.31*	**5.63** ± *2.74*		**0.71** ± *0.01*	**0.29** ± *0.01*
40	**9.28** ± *0.08*		**10.1** ± *0.29*	**3.94** ± *0.72*		**0.7** ± *0.06*	**0.3** ± *0.06*
50	**6.36** ± *0.14*		**7.44** ± *0.49*	**3.66** ± *0.28*		**0.56** ± *0.08*	**0.44** ± *0.08*

Temp, temperature, I τAV, intensity weighted average lifetime (ns); α, fractional amplitudes. 1 mol% of the fluorescent probes tPA-SM (partitions to ordered domains) or O-tPA-PC (partition to disordered domains) was included in the bilayers. Multilamellar vesicles were prepared with the composition PSM/POPC/POPE/POPS 22:44:17:17 with and without 31 mol% cholesterol.

References

1. Terova, B., J. P. Slotte, and T. K. Nyholm. 2004. Miscibility of acyl-chain defined phosphatidylcholines with N-palmitoyl sphingomyelin in bilayer membranes. Biochim. Biophys. Acta 1667: 182-189.

2. Rouser, G., S. Fkeischer, and A. Yamamoto. 1970. Two dimensional thin layer chromatographic separation of polar lipids and determination of phospholipids by phosphorus analysis of spots. Lipids 5: 494-496.

3. Jungner, M., H. Ohvo, and J. P. Slotte. 1997. Interfacial regulation of bacterial sphingomyelinase activity. Biochim Biophys Acta 1344: 230-40.

4. Kuklev, D. V., and W. L. Smith. 2004. Synthesis of four isomers of parinaric acid. Chem Phys Lipids 131: 215-222.

5. Bjorkqvist, Y. J., J. Brewer, L. A. Bagatolli, J. P. Slotte, and B. Westerlund. 2009. Thermotropic behavior and lateral distribution of very long chain sphingolipids. Biochim. Biophys. Acta 1788: 1310-1320.

6. Huang, C., and J. T. Mason. 1986. Structure and properties of mixed-chain phospholipid assemblies. Biochim Biophys Acta 864: 423-470.

7. Sklar, L. A., B. S. Hudson, and R. D. Simoni. 1977. Conjugated polyene fatty acids as fluorescent probes: synthetic phospholipid membrane studies. Biochemistry 16: 819-828.

8. Davis, J. H. 1983. The description of membrane lipid conformation, order and dynamics by 2H-NMR. Biochim. Biophys. Acta 737: 117-171.

9. McCabe, M. A., and S. R. Wassail. 1997. Rapid deconvolution of NMR powder spectra by weighted fast Fourier transformation. Solid State Nuclear Magnetic Resonance 10: 53-61.

10. Halling, K. K., B. Ramstedt, J. H. Nystrom, J. P. Slotte, and T. K. Nyholm. 2008. Cholesterol interactions with fluid-phase phospholipids: effect on the lateral organization of the bilayer. Biophys. J. 95: 3861-3871.